Utrecht University

Department of Earth Sciences

Master's Thesis

July 1, 2015

Mantle dynamics on Venus: insights from numerical modelling

Iris van Zelst

1st *Supervisor:*
Dr. A.P. van den Berg
Department of Earth Sciences, Utrecht University, Utrecht, The Netherlands

2nd *Supervisor:*
Dr. R.C. Ghail
Department of Civil and Environmental Engineering, Imperial College London, London, United Kingdom

3rd *Supervisor:*
Dr. C. Thieulot
Department of Earth Sciences, Utrecht University, Utrecht, The Netherlands

Abstract
Numerical modelling studies of the various hypotheses of Venus' thermal evolution, such as the uniformitarian, catastrophic, differentiated planet hypothesis have been conducted. However, these studies often failed to investigate the influence of the mantle thickness and core-mantle boundary temperature on their results. As these parameters are not very well constrained, a modelling study was conducted to assess their influence. Besides that, the influence of the rarely used temperature-dependent conductivity was investigated and the first numerical validation of the subcrustal lid rejuvenation hypothesis was conducted. A two dimensional, Cartesian, square box was used with free slip boundary conditions and isothermal top and bottom boundaries. A temperature dependent viscosity with the inclusion of a yield stress was used. It was found that the mantle thickness determines whether or not a periodic regime can be accommodated: a thin mantle cannot result in a periodic regime. To a lesser extent, the core-mantle boundary temperature influences this as well. This is particularly the case, when it is combined with the temperature-dependent conductivity, which causes the periodic regime to be stable over a larger range of yield stresses. In order to obtain more realistic models in the future, additional heat sources should be added to the model in the form of shear heating, adiabatic heating and internal heat production.

Keywords: Venus, mantle convection, lid rejuvenation, temperature-dependent conductivity

Contents

1. Introduction

Venus is the neighbour of Earth that is closest to the Sun. The two planets are very similar in size, mass and average density (see Table 1). However, despite their similarity Venus and Earth are very different at present. For example, the Earth has a magnetic field, while Venus appears to have none. Besides that, Earth displays plate tectonics, while Venus does not. Furthermore, Venus spins backwards, compared to Earth as well as very slowly (the duration of one Venus day is ~ 243 Earth days (Mueller et al., 2012)). These differences indicate a different evolution of the planets. Whether or not this is solely due to Venus' closer proximity to the Sun remains at present unclear and is hard to quantify. Insights into the evolution of Venus could provide new insights on why Earth is a unique planet that supports life along with insights into the general evolution of terrestrial planets.

Table 1: A comparison between Earth and Venus[1]

	Venus	Earth
Radius (m)	6.0518×10^6	6.3710×10^6
Mass (kg)	4.8673×10^{24}	5.9722×10^{24}
Density (kg m^{-3})	5243	5513

In order to obtain insights in the evolution of Venus, data has been collected and analyzed from space missions and Earth-based observations. These observations in turn triggered the development of various hypotheses concerning the different stages of the evolution of Venus. In order to determine whether these hypotheses can accurately reproduce the data, Monte Carlo simulations, analytical solutions and numerical models have been used.

In this work an overview is presented of the observations of Venus from space missions and the subsequent hypotheses regarding the evolution of Venus, focusing on the evolution of its mantle dynamics. In order to contribute to the current literature on mantle dynamic models, a modelling study is conducted to

[1] http://solarsystem.nasa.gov/planets/profile.cfm?Object=Earth&Display=Facts
http://solarsystem.nasa.gov/planets/profile.cfm?Object=Venus&Display=Facts

Table 2: Measurements of surface temperature and pressure

Space mission	Temperature (K)	Pressure (MPa)	Reference
Venera 4, 5, 6	770 ± 60	$9.8^{+4.7}_{-2.0}$	Avduevsky et al. (1970)
Venera 7	747 ± 20	8.8 ± 1.5	Avduevsky et al. (1971)
Venera 8	743	9.1	Vinogradov et al. (1973) (no uncertainties available)
Venera 9, 10	735 ± 5	9.2 ± 0.3	Florensky et al. (1977)

investigate the influence of the mantle thickness and the core-mantle boundary temperature on the mantle convective regime, as these parameters are at present unknown. Furthermore, the influence of a temperature- and pressure-dependent conductivity is investigated and a new hypothesis is tested, as no previous modelling studies have looked into that yet (see Section 6).

2. Past missions to Venus

Venus is completely covered in clouds, so information about the surface of the planet cannot be obtained directly from Earth-based measurements. Hence, space missions to Venus are required in order to study the surface of Venus, and from that the activity and dynamics of Venus. In this section an overview of the past space missions to Venus and their contribution to our present-day understanding of Venus is presented.

2.1. Venera missions

The Russian Venera 1 - 16 probes were launched from 1961 to 1984 with varying degrees of success to gather data from Venus. Venera 1 and 2 were designed as flybys, but failed to send data to Earth. Venera 3 - 6 orbiters were designed to investigate the atmosphere of Venus. After the failure of Venera 3, Venera 4 - 6 succeeded in measuring some physical and chemical characteristics of the Venusian atmosphere. For example, the composition of the atmosphere was estimated (see Table 3 (Vinogradov et al. (1968) and Avduevsky et al. (1970))). Venera 4 also investigated the presence of a magnetic field on Venus. The results from this experiment could indicate either magnetization of the ionosphere or an intrinsic magnetic dipole moment which corresponds to a surface field of 30×10^{-9} T (Russell, 1976). In comparison, Earth's magnetic field at the surface has a magnitude of 50×10^{-6} T (Glassmeier et al., 2008). Extrapolation of the temperature and pressure measurements of Venera 4 - 6 resulted in the first empirical estimate of the surface temperature and pressure on Venus (see Table 2).

Venera 7 deployed a probe designed to withstand the surface conditions on Venus, that landed on the surface of Venus (see Figure 1) on December 15, 1970 (Avduevsky et al., 1971). The descent of the probe through the atmosphere resulted in vertical temperature and pressure profiles of the Venusian atmosphere, leading to better estimates of the surface temperature as shown in Table 2.

Table 3: Atmospheric composition as measured by Venera 4 - 6 at P = 0.6 MPa (Vinogradov et al. (1968) en Avduevsky et al. (1970))

Species	Percentage (%)
CO_2	95 ± 2
N_2	3.5 ± 1.5
H_2O	0.4 ± 0.2
O_2	< 0.4

Venera 8 measured both wind velocities and the temperature in a vertical profile of the Venusian atmosphere, and deployed a lander as well. The wind speeds were found to be 15 - 40 m s^{-1} between 40 and 20 km altitude with a decrease in wind speed around 15 km altitude. Vertical winds of 2 - 5 m s^{-1} were found at 20 - 30 km altitude. Surface winds on Venus are 0.1 m s^{-1} or less (Ainsworth and Herman, 1975). The gamma ray spectrometer on board of the lander of Venera 8 measured the content of radioactive potassium, uranium, and thorium on the surface of Venus (see Table 4 and Figure 1 for the location of the landing site). Vinogradov et al. (1973) interpreted this as a granitic composition and concluded that Venus must be a differentiated planet like Earth.

Table 4: Abundance of radioactive elements in rocks at the Venera 8 lander site (Vinogradov et al., 1973)

Species	Weight percentage (%)
K	4.0 ± 0.2
U	$(2.2 \pm 0.4) \times 10^{-4}$
Th	$(6.5 \pm 0.3) \times 10^{-4}$

Venera 9 and 10 both contained landers as well, so new estimates of the surface temperature and pressure were obtained (see Table 2 and Figure 1). The wind velocities that were measured were 0.5 to 1 m s^{-1}. The rocks that the landers were able to analyze were found to be similar to Earth's basalt in radioactive content. The density of the rocks was measured to be 2800±100 kg m^{-3} (Florensky et al., 1977).

The landers of Venera 11 and 12 (see Figure 1) both gathered more detailed information on the Venusian atmosphere. New information regarding the rocks on Venus was obtained by Venera 13 and 14 (see Figure 1), as these missions were able to determine the elemental composition of the rocks. The chemical composition of the rock that was analyzed by Venera 13 was similar to the potassium alkaline basalts commonly found in rift zones and on oceanic islands on Earth (Surkov et al., 1983). The rocks analyzed by Venera 14 had a composition similar to that of tholeiitic basalts of the oceanic crust on Earth (Surkov et al., 1983). Measurements of the physical and mechanical properties of the rocks showed that the Venusian rocks consist of weakly cemented, porous structures (Surkov et al., 1984). Based on the data from Venera 8, 9, 10, 13 and

14, Surkov et al. (1984) concluded that the rocks on Venus are most likely formed during volcanic eruptions.

Besides analyzing rock samples, Venera 13 and 14 also took panoramic photographs of their landing sites. An analysis of these photographs, as conducted by Florensky et al. (1983) indicated the presence of ripple marks, thin layering and differential erosion on the surface of Venus. Some of the visible formations were interpreted as lithified clastic sediments (Florensky et al., 1983).

The next step in the Venera missions was to image the surface and to measure the altimetry. Therefore, Venera 15 and 16 both had radar imaging equipment on board, in addition to Fourier spectrometers to measure the atmospheric composition of the top cloud level (Oertel et al., 1985). Venera 15 and 16 did not map the entire surface of Venus. From the radar imagery and altimetry measurements, the distribution of impact craters could be studied, leading to estimates of the age of the surface of Venus and hypotheses on the tectonics of Venus (see Section 3.2 and Section 5.5).

2.2. *Pioneer Venus*

The Pioneer Venus project by NASA consisted of 2 missions, namely the Pioneer Venus Orbiter and the Pioneer Venus Multiprobe.

The Pioneer Venus Orbiter was launched in May 1978 and was designed to study the atmosphere of Venus as well as the topography, surface characteristics and gravity field. The Pioneer Venus Orbiter mapped 93% of the surface of Venus with a surface resolution higher than 150 km and the vertical accuracy exceeded 200 m (Pettengill et al., 1980). The gravity and altimetry data indicate that the observed highlands, such as Ishtar Terra and Aphrodite Terra, are isostatically balanced (see Section 3 and Figure 1) (Masursky et al., 1980).

The atmospheric experiments resulted in the discovery of a decrease in SO_2 concentration in the top clouds in the period 1978 - 1986 (Esposito et al., 1988). Esposito et al. (1988) explained this behaviour by proposing episodic injection of SO_2 into the atmosphere. This could be caused by active volcanism.

The Pioneer Venus Multiprobe was launched in August 1978 and designed to study the atmosphere of Venus. Apart from a large probe that carried seven experiments to study the atmospheric composition and particles, three identical small probes, the North probe, the Night probe and the Day probe, targeted different parts of Venus to measure regional variations in atmospheric composition. One of the results was the presence of three different cloud regions at an altitude of $\sim$ 49 km (Tomasko et al., 1979).

2.3. *Vega*

The Russian Vega program consisted of two sister spacecrafts, Vega 1 and Vega 2, that were launched in 1984 on December 15 and 21, respectively. The Vega mission was designed to study both Venus and the comet Halley that appeared in 1986. The Vega mission deployed two balloons in the atmosphere to measure the temperature, the pressure, the velocity of vertical winds, the backscatter of cloud particles, the ambient light level, and the frequency of lightning in situ (Sagdeev et al., 1986). In order to further study the composition of rocks on the surface of Venus, landers identical to those of the Venera missions were used. The lander of Vega 1 landed in the Mermaid Valley and the lander of the Vega 2 mission landed on the previously unanalyzed northeastern slope of the Aphrodite Terra (see Figure 1 for the landing sites) (Surkov et al., 1986). Based on the content of radioactive elements in the rocks, it was found that the rocks are similar to basic rocks (mostly tholeiitic basalts and gabbros) of the Earth's crust (Surkov et al., 1987). The analyzed rocks at the Vega 2 site were interpreted more specifically as being olivine gabbro-norite (Surkov et al., 1986).

2.4. *Magellan*

The Magellan spacecraft was launched on May 4, 1989. Its main objective was to map the surface of Venus with a synthetic aperture radar and to measure the gravity field of Venus. A variety of deformational features was imaged by Magellan, such as families of graben, wrinkle ridges, ridge belts, mountain belts, quasi-circular coronae and broad rises with linear rift zones with dimensions of hundreds to thousands of kilometers (see also Section 3.3) (Solomon et al., 1992). These last two deformation styles are not observed on Earth and appear to be unique to Venus. The mapping of Magellan also resulted in a detailed knowledge of the distribution of impact craters, which is indistinguishable from random (also see Section 3.2).

The images from Magellan confirm that the surface of Venus is probably volcanic, based on the photographs and geochemical data from the Venera and Vega missions (Kargel et al., 1993). More specifically, the data are consistent with mafic and basaltic compositions of the rocks (Head et al. (1992) and Kargel et al. (1993)).

2.5. *Venus Express*

Venus Express (ESA) was the first European mission to Venus and was designed to investigate the atmosphere, the plasma environment and the surface of Venus from orbit (e.g., Titov et al. (2006) and Svedhem et al. (2007)). Venus Express was launched on 9 November, 2005 (Svedhem et al., 2007). One of the instruments aboard was the Visible and Infrared Thermal Imaging Spectrometer (VIRTIS), designed to investigate the atmospheric properties of Venus as well as optical surface properties (Drossart et al., 2007). The spectral emissivity measured by VIRTIS was used to determine the chemical composition of the surface of Venus and to study likely candidates for hotspots on Venus. Due to anomalously high thermal emissivity values, Smrekar et al. (2010) identified compositional differences in lava flows at three different locations that are potential hotspots: Imdr, Themis, and Dione Regiones (see Figure 1). The interpretation of these compositional differences is a lack of weathering, thereby indicating that the lava flows are relatively young (Smrekar et al., 2010). The age of the lava flows was determined to be younger than 2.5 Myr and possibly even younger than 250.000 years (Smrekar et al., 2010). This indicates that Venus is at present volcanically active (see also Section 3.2 and 5).

The Venus Monitoring Camera was used for thermal mapping of the surface (Markiewicz et al., 2007). Bright features that appeared and disappeared in the time span of a few days in the Ganiki Chasma (see Figure 1) were interpreted as being the result of the presence of hot matter at or just above the surface (Shalygin et al., 2014). This could be lava, gas or a combination of both.

Like the Pioneer Venus Orbiter, the Venus Express mission provided information about the SO_2 concentration in the clouds of Venus with the use of the Spectroscopy for Investigation of Characteristics of the Atmosphere of Venus (SPIVAC) instrument (Marcq et al., 2013). Again, a decrease in SO_2 concentration was measured in the period 2007 - 2012 (Marcq et al., 2013). Besides that, Marcq et al. (2013) found latitudinal and temporal variations in the abundance of SO_2. As a cause for these episodic SO_2 injections, Marcq et al. (2013) suggested active volcanism with, more specifically, periods of increased buoyancy of the volcanic plumes. If there is no active volcanism on Venus, the SO_2 concentrations over time can be explained by long-period oscillations of the general atmospheric circulation.

In summary, past missions have provided a wealth of information about present-day Venus. The surface temperature and pressure have been determined accurately; the surface of Venus has been mapped; and rocks on the surface of Venus have been sampled. Data from the missions indicate a mafic (or basaltic) composition of the surface of Venus. Indications for active volcanism are present from emissivity data, thermal mapping and SO_2 abundances in the atmosphere.

3. Observations of the surface of Venus

The interpretation of the observations of the various missions to Venus provides information on the history and current state of the planet. In this section, the results of the global mapping measurements, which resulted in information regarding the topography, gravity and impact crater distribution are discussed.

3.1. Global topography & gravity

In this section the topography and gravity maps of Venus are presented. Besides that, several hypotheses that could explain the topography and gravity distribution and their correlation are discussed.

3.1.1. Topography

The radar altimetry measurements made during the first 8 months of the Magellan mission were analysed by Ford and Pettengill (1992). It was found that the surface heights exhibit a unimodal distribution, where more than 80% of the surface lies within 1 km of the mean radius of 6051.84 km. Several steep features with slopes greater than 30° were found on the southwest face of the Maxwell Montes, the southern face of the Danu Montes and the chasmata to the east of the Thetis regio (see Figure 1). This is also confirmed by the synthetic aperture radar measurements.

Another topography model was made by Rappaport et al. (1999) (see Figure 1), who used the altimetry measurements in combination with a gravity model from which the spacecraft position was derived in detail. From the topography distribution it can be concluded that Venus consists of only one plate at present (Schubert et al., 2001). However, there are features evident from the topography that resemble tectonic features on Earth. Regions that portray rift zone characteristics are the Beta, Atla, Eistla and Bell Regiones (see Figure 1) (Schubert et al., 2001). An example of a major collision zone, such as the mountain belt that links the Alps and the Himalayas, is the Aphrodite Terra. Another feature is the Ishtar Terra (see Figure 1), which is as large as 2000 - 3000 km in length. It is a region of elevated topography with the Lakshmi Plateau (see Figure 1) as its major feature. This plateau is similar to the Tibetan Plateau, with a mean elevation of 4 km (Schubert et al., 2001). Like the Tibetan Plateau, the Lakshmi Plateau is surrounded by mountain belts similar to the Himalayas: the Akna, Danu, Freyja and Maxwell Montes reach elevations of ~10 km (see Figure 1).

To explain the high topography on Venus, two main hypotheses were put forward according to Schubert et al. (2001). The first hypothesis *(1)* is that the high topography on Venus is compensated by crustal roots, following the Airy model of isostasy for Earth (Schubert et al., 2001). The other hypothesis *(2)* is that the interaction of mantle convection with the lithosphere is responsible for the high topography. This is also called dynamic topography. An example of this are the equatorial highlands on Venus (excluding the Ovda and Thetis Regiones), which are generally associated with upwellings in the mantle (Schubert et al., 2001).

An example of a model combining these two hypotheses in order to explain the topography of Venus is given by Morgan and Phillips (1983). They show that 93% of surface topography of Venus can be explained by variations in lithospheric thickness (hypothesis *(1)*). If the assumption is made that crust forms at hot spots (a version of hypothesis *(2)*), the model corresponds to the surface topography for 99%.

Hence, even though Venus appears to be a one-plate planet at present, there are topographic features indicating tectonics. The precise cause of the high topography is at present uncertain.

3.1.2. Gravity

In 1981 part of the gravity field of Venus was determined for the first time from Doppler tracking data of the Pioneer Venus Orbiter (Dickey et al., 1997). The raw Doppler tracking data was corrected for many known effects on the radio signal, such as the rotation of the Earth, the orbital motion of the spacecraft, planetary pertubations, relativity and the atmosphere of Venus (Sjogren et al., 1983). The filtered data provided information about the gravity field because the position of the spacecraft depends on the local gravity field of Venus. These first estimates of the gravity field showed a very high ratio between geoid and topography compared to Earth. This lead to estimates of the compensation depths of the topography of approximately 100 km or more (Dickey et al., 1997).

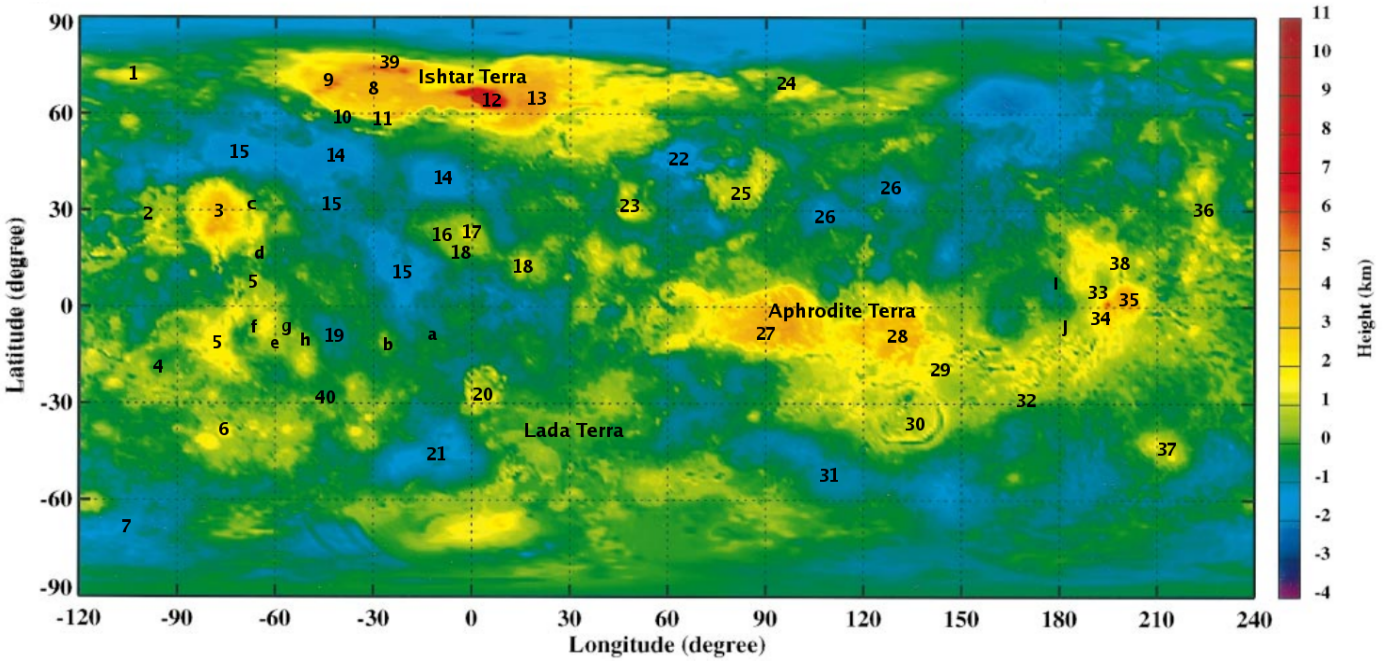

Figure 1: Topographic map of Venus, modified from Rappaport et al. (1999). The three terras of Venus are indicated. Other topographic regions are indicated by numbers: 1. Metis Regio; 2. Asteria Regio; 3. Beta Regio; 4. Phoebe Regio; 5. Devana Chasma; 6. Themis Regio; 7. Helen Planitia; 8. Lakshmi Planum; 9. Akna Montes; 10. Vesta Rupes; 11. Danu Montes; 12. Maxwell Montes; 13. Fortuna Tessera; 14. Sedma Planitia; 15. Guinevere Planitia; 16. Sif Mons; 17. Gula Mons; 18. Eistia Regio; 19. Navka Planitia; 20. Alpha Regio; 21. Lavinia Planitia; 22. Leda Planitia; 23. Bell Regio; 24. Thetus Regio; 25. Tellus Tessera; 26. Niobe Planitia; 27. Ovda Regio; 28. Thetis Regio; 29. Diana Chasma; 30. Artemis Chasma; 31. Aino Planitia; 32. Dali Chasma; 33. Ozza Mons; 34. Maat Mons; 35. Atla Regio; 36. Ultrum Regio; 37. Imdr Regio; 38. Ganiki Chasma; 39. Freyja Montes; 40. Dione Regio. Landing sites of space missions are indicated by letters: a. Venera 7; b. Venera 8; c. Venera 9; d. Venera 10; e. Venera 11; f. Venera 12; g. Venera 13; h. Venera 14 i. Vega 1; j. Vega 2.

A more recent model of the gravity field of Venus was made in 1999, when Konopliv et al. (1999) incorporated data from Doppler tracking of the Magellan spacecraft to obtain the global gravity field. Following from that, Konopliv et al. (1999) developed a 180 degree spherical harmonics model for the geoid of Venus, which is shown in Figure 2. Notable areas with high positive gravity anomaly include the Beta and Atla Regio (see also Figure 1).

3.1.3. Correlation topography and gravity

Comparing Figures 1 and 2 shows that the topography and gravity anomalies on Venus seem to correlate, in contrast to Earth. More quantitatively, Konopliv et al. (1999) correlated the geoid and topography for different spherical harmonic degrees. For spherical degrees 120 to 150, it was found that there is a high correlation near the Beta Regio (>0.8) and the Atla Regio (~0.8) (see Figures 1 and Figure 2). Other regions of high correlation (~0.5) are the Ishtar Terra and the eastern Eistla Regio. For higher spherical degrees of 150 to 180 the Beta Regio again shows the highest correlation, together with parts of the Atla and eastern Eistla Regiones.

In order to explain the correlation between topography and gravity, Sjogren et al. (1983) speculated that the different topography-gravity ratios could reflect differences in internal density distribution or topographic compensation depth.

Simons et al. (1997) relied on the two main hypotheses for topography. Simons et al. (1997) suggested that the data from the highland plateaus and tessera regions is consistent with isostatic compensation of the topography by variations in the thickness of the crust (hypothesis *(1)*). The maximum thickness of the crust in these regions was estimated to be 40 km maximum. The topography-gravity correlation of the other regions, which mainly comprise rises, plains and lowlands, are probably the result of mantle tractions at the base of the lithosphere (hypothesis *(2)*) (Simons et al., 1997).

In summary, the high topography on Venus correlates with large gravity anomalies. Proposed explanations for this include isostatic compensation and dynamic topography. Although combinations of these can account for up to 99% of the surface topography, the gravity cannot be explained fully. Therefore, at present there is no model that can explain both the gravity and topography distribution on Venus.

3.2. Age of the surface

Knowledge about the age of the surface of Venus is important in order to obtain some constraints on the evolution of Venus. As an example, a smooth and relatively young surface would indicate some form of repetitive crust renewal. The mapping of the surface of Venus, and the resulting impact crater distribution that was discovered by various missions, therefore lead to estimates of the age of the surface of Venus. In this section these estimates are discussed.

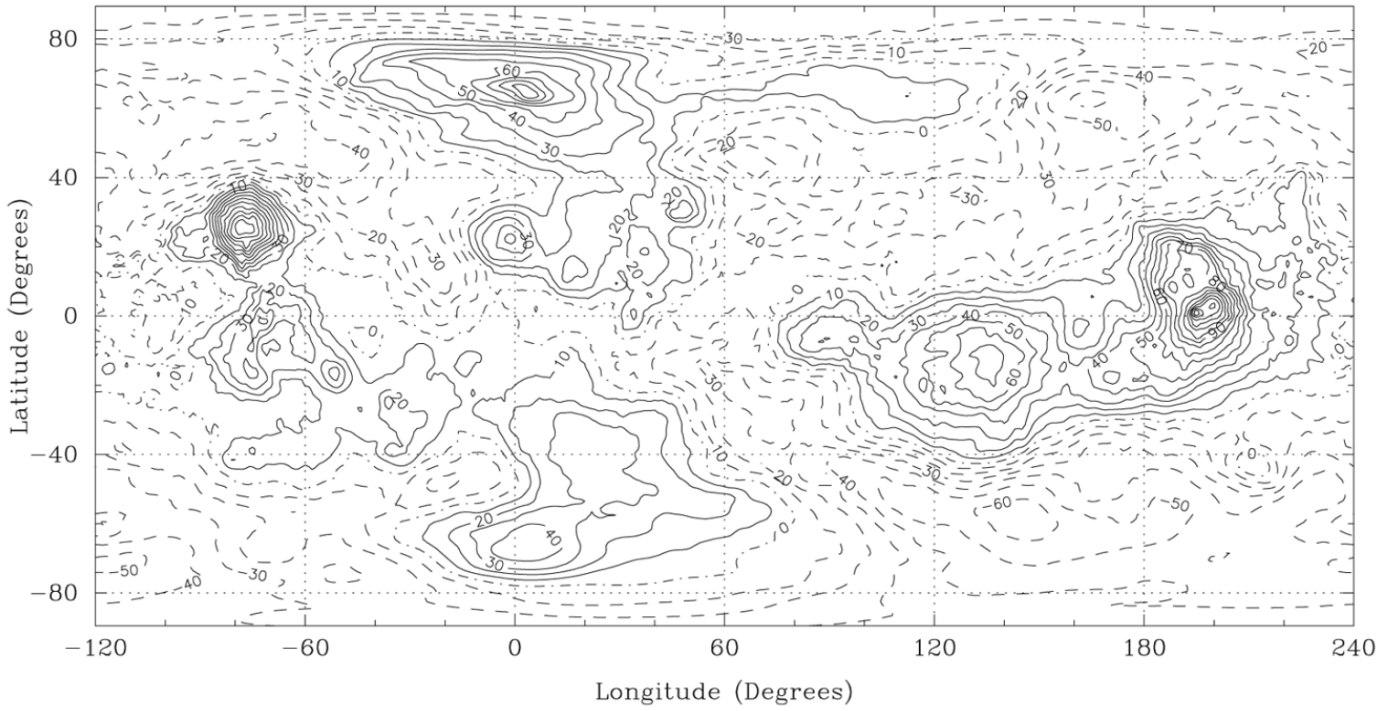

Figure 2: Geoid of Venus with respect to a reference sphere, from Konopliv et al. (1999). Contours are at 10 m intervals.

One of the first studies that tried to determine the age of the surface was conducted by Schaber et al. (1987), who interpreted the data from the Venera 15 and 16 missions. As these missions only mapped about 25% of the surface, the results from Schaber et al. (1987) were preliminary. Based on the assumption that the cratering rate on Earth and Venus is similar for craters ≥ 20 km and taking into account the uncertainty in the history of impact craters on Earth, Schaber et al. (1987) concluded that the average age of the surface of Venus could be as great as 450 Myr.

In a follow-up study, Schaber et al. (1992) studied the data from Magellan, which mapped a larger portion of the Venusian surface (89%) in higher resolution than the Venera missions. Schaber et al. (1992) identified 842 craters on Venus' surface ranging from 1.5 to 280 km in diameter. By studying the size-density distribution of the craters, Schaber et al. (1992) found that the average age of the surface is approximately 500 Myr. Here, the density distribution of impact craters is defined as (Price and Suppe, 1994):

$$\rho = \frac{n}{A} \tag{1}$$

where n is the number of impact craters in the area A which is considered. Schaber et al. (1992) interpreted this result as an indication of one or more resurfacing events that erased the planet's cratering record of which the last ended 500 Myr. Schaber et al. (1992) argued that the amount of volcanic activity declined after this resurfacing event.

In contrast to this, Zahnle and McKinnon (1996) found an age of the surface of Venus of 800^{+800}_{-400} Ma. A more recent study, conducted by Korycansky and Zahnle (2005), showed that the age of the surface of Venus is 740±110 Myr, using Monte Carlo methods and cratering distributions.

The aforementioned studies all assumed a global uniform surface age. However, the surface age does not necessarily have to be uniform. Hansen and Young (2007) looked at the impact craters in detail, and observed that the morphological characteristics are indicative of deterioration of the impact crater. With this observation, Hansen and Young (2007) were able to divide impact craters in age groups, where old craters have smooth interiors and degraded annuli (Hansen and Young, 2007).

It was found that several regions of different age can be identified based on their impact crater density. When this age division is taken into account, it seems that the lowlands are generally associated with old surface age regions (Herrick and Phillips, 1994). The crustal plateaus are generally located in the intermediate age regions. The regions where possible tectonic or volcanic activity has been proposed lie in the young surface age regions. The reason for this age distribution is at present still unclear. Possible explanations are discussed in Section 5.

Some impact craters also have specific features such as dark haloes, bright floors and parabolic features. The age for these types of craters was calculated by Herrick and Phillips (1994), which resulted in an age of 140, 80 and 30 Ma, respectively. In line with this, Herrick and Rumpf (2011) showed that impact craters experienced postimpact tectonic deformation or volcanism by studying stereo-derived topography. This implies that resurfacing histories that are based on the assumption that impact craters are at the top of the stratigraphic column are

invalid (see also Section 3.3.2 and 5). From their new results on postimpact deformation, Herrick and Rumpf (2011) postulated a young mean surface age of Venus of approximately 150 Myr.

Other studies focused on the age of specific regions, in order to determine whether Venus is currently active or not. Price and Suppe (1994) found that there is a low impact crater density on large volcanic structures compared to the average crater density on the surface of Venus. Because of this, Price and Suppe (1994) addressed the question whether this observation was a random distribution of craters after the global resurfacing event, which Price and Suppe (1994) date 300 - 500 Myr ago, or whether it was due to the ongoing tectonics and volcanism on Venus. By using Monte Carlo tests to calculate the density distributions for randomly generated point sets, it was found that the probability that the impact crater density in an area is random is less than 0.015. From this, Price and Suppe (1994) conclude that volcanic and tectonic activity younger than the global resurfacing event altered the crater density. In line with this, Price and Suppe (1994) estimated the ages of several features indicating volcanic activity: the mean age of volcanoes, lava flood fields, coronae (see Section 3.3.1) and rifts was found to be 70 - 125 Ma. This indicates that volcanic and tectonic activity indeed continued after the global resurfacing event and that Venus is probably an active planet at present (Price and Suppe, 1994). In line with this, Basilevsky (1993) estimated the age of rifting and volcanism in the Atla Regio on Venus based on the previous study by Schaber et al. (1992). Basilevsky (1993) used information deduced from impact craters and stratigraphy based on photogeologic analyses. It was found that the rifting and its associated volcanism in the Alta Regio were recently active during the last ~50 Myr.

However, Zahnle and McKinnon (1996) argued that Venus is most likely a non-active planet. The reason for this is their estimate of Venus' surface age: if the surface of Venus is indeed only 400 Myr old, the global resurfacing event had to have occurred reasonably fast, in 50 Myr or less, because otherwise the relative ages would have been apparent in the impact crater distribution. On the other hand, if the surface of Venus is 800 Myr old, a global resurfacing event of approximately 100 Myrs is possible. Zahnle and McKinnon (1996) argued that when the time since the last resurfacing event increases, the likelihood that Venus is now in between resurfacing events diminishes. Therefore, Zahnle and McKinnon (1996) conclude that it is likely that Venus is a non-active planet.

In summary, there remains an inconsistency between different studies as to the exact age of the surface of Venus. The reason for this is that the crater distribution as mapped by various missions can be interpreted differently in terms of the number of impactors. Besides that, the variety of Monte Carlo methods that were used all have different advantages and limitations concerning the different scenarios that they take into account. Furthermore, some studies try to discern the surface age from isolated impact craters studies, without taking into account the geological evidence. However, most models agree that a resurfacing event occurred on Venus 800 – 300 Myr ago regardless of whether Venus is active at present or not.

3.3. Regional observations

In addition to the global mapping of the various space missions that lead to a general understanding of the topography, gravity and surface age, many regional and smaller scale observations were made as well. These observations were mainly the result of the detailed mapping of the Magellan mission. In this section, the surface features unique to Venus are described, as are the most notable regional observations.

3.3.1. Surface features unique to Venus

The mapping cycles of the Magellan mission allowed for the discovery of many surface features also found on Earth, such as volcanoes, mountains, rift valleys and aeolian structures. However, several surface features that were discovered from the images from Magellan bore no direct resemblance to structures on Earth. In fact, they appeared to be unique to Venus. In the following, the surface features that are unique to Venus, the tesserae and the coronae, are described and possible mechanisms of their formation are discussed.

The tessera regions are highly deformed regions characterized by multiple tectonic lineaments (see Figure 3a)(Hansen et al., 1999). Usually they are exposed in crustal plateaus (Hansen et al., 1999). The mechanism of the formation of the tesserae remains at present unclear, but several hypotheses have been proposed. For example, Hansen et al. (1999) proposed that the thickened crust of the tesserae is caused by the interaction between mantle plumes or downwellings and thin Venusian lithosphere. More recently, Hansen (2006) proposed the lava-pond hypothesis. The lava pond hypothesis explains the crustal plateau formation of tesserae with the solidification of a huge lava pond. The lava pond could in turn be the result of a large bolide (a diameter of 20 - 30 km) that impacted with the lithosphere (Hansen, 2006).

Coronae are pancake like, oval-shaped volcanic features (see Figure 3b). Their size ranges from 60 - 2000 km diameter (Stofan et al., 1992). The annulus around the coronae (which gives it a crown-like appearance) ranges from 10 - 150 km in diameter. The tectonic features associated with these annuli can be extensional, compressional or both. Morphologically, coronae are similar to large shield volcano structures (Stofan et al., 1992). Stofan et al. (1992) noted that the spatial distribution of coronae is not random. Instead, the coronae are found in clusters and chains. The largest corona on Venus is Artemis in the Aphrodite Terra (see Figure 1 and 3b). Similar to the tesserae, the origin of coronae is not clear. Most hypotheses centre around the general idea that coronae are the result of mantle plumes (Stofan et al., 1992), but the details of the hypotheses vary (see also Section 6.3). One of the reasons for this is that different coronae could have different modes of origin. More specifically, the larger coronae such as the Artemis corona probably had a different formation mechanism than the smaller coronae that likely overlie sill-like intrusions.

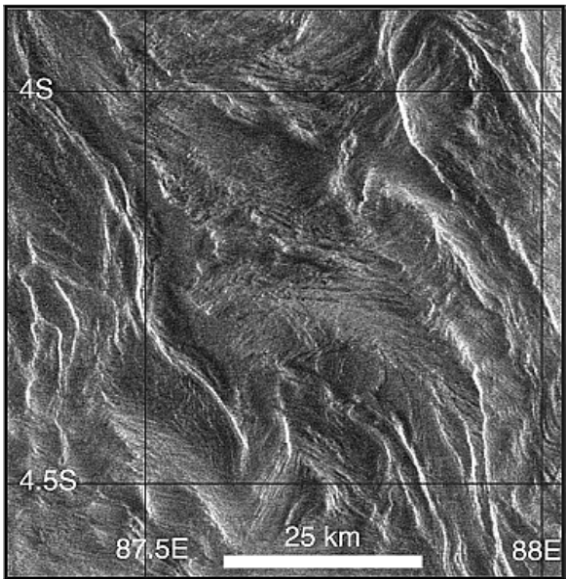

(a) Tessera in Ovda Regio

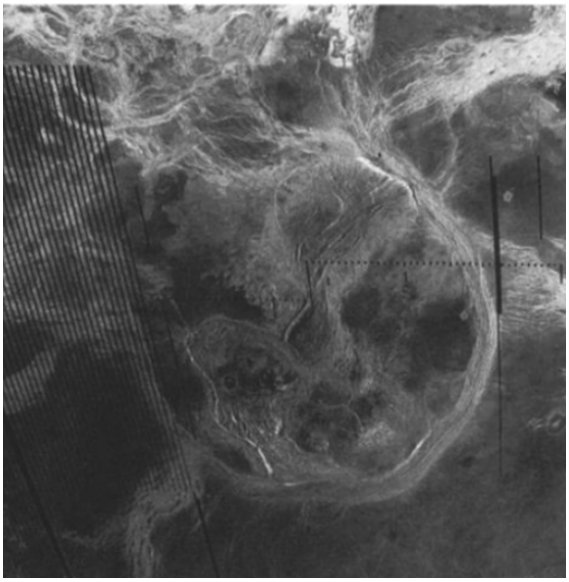

(b) Artemis corona

Figure 3: Figure (**a**) from Hansen (2006) and figure (**b**) from Stofan et al. (1992). Examples of surface features unique to Venus: (**a**) a Synthetic Aperture Radar image of a tessera region in the Ovda Regio with indicated scale and (**b**) an image from Magellan of the Artemis corona with a diameter of 2600 km. See Figure 1 for the locations on the map of Venus of these features.

A feature that is not unique for Venus is the so-called wrinkle ridge. Wrinkle ridges are tectonic, ridge-like features that can extend for hundreds on kilometers. They are formed when the surface, which for example consists of lava or sediments, cools and contracts. On Venus, wrinkle ridges occupy approximately 43% of the plains (Bilotti and Suppe, 1999). The correlation between wrinkle ridges, plains and lows in the geoid suggest that they could overlie regions of downwelling or delamination (Ghail, 2015). On Earth wrinkle-ridges are also present, although they are then generally referred to as reverse normal structures. Apart from Venus and Earth, these features are also found on the Moon, Mars and Mercury (Watters, 1988).

3.3.2. Detailed observations from Magellan

Through studying the detailed images from Magellan, several noticeable observations were made. In this section, the observations most relevant to the tectonic activity and the mantle processes on Venus are discussed. Moreover, hypotheses on the tectonics or the mantle convective regime of Venus should be able to explain these features (see Section 5).

According to Hansen and Young (2007) most impact craters on the surface of Venus are relatively pristine. In other words, few of the impact craters are flooded or faulted. According to Hansen and Young (2007) this could indicate that the mechanism of destruction of impact craters on Venus results in complete destruction of the impact craters beyond recognition. This interpretation of the radar images from Magellan is in direct contrast with the study from Herrick and Rumpf (2011), who argued that impact craters experienced postimpact volcanism and tectonic deformation (see Section 3.2). So, although the images from Magellan provide a valuable source of data, the interpretation of them can vary significantly.

It has been shown by numerous studies (see Hansen and Young (2007) and references therein) that thin layers or lava flows cover the extensive lowland regions. In contrast, the lava flows required to completely bury an impact crater should be approximately 650 m thick, based on the height of the annuli of impact craters (Hansen and Young, 2007).

Another noticeable observation is that the pristine impact craters are located on top of tesserae, indicating that the impact craters are younger than the deformation of the tesserae (Hansen and Young, 2007). However, it is difficult to distinguish between pristine craters and subsequent (partial) tectonic alteration, because the structures of the fracture zone may be influenced by the highly damaged zone around impact craters. Taking into account the study of Herrick and Rumpf (2011), it might even very well be that the impact craters are not at the top of the stratigraphic column.

Besides being noticeable observations, it is important that hypotheses that try to explain the evolution of Venus can explain these detailed, regional observations as well. The different interpretations of the data can however lead to different models. Possible hypotheses are discussed in Section 5.

4. Constraints on the interior of Venus

By using the direct measurements of the surface of Venus, information about the interior of Venus can be obtained. Most studies that were based on direct observations focused on the composition and size (or thickness) of the crust and core. Because the bulk density and radius of Venus are known, characteristics of the mantle can be deduced by combining the various data sets concerning the crust and core. In this section the constraints on the crust and core of Venus that are supported by

data are discussed.

4.1. The crust

Both the thickness and the density of the crust can provide an indication of the amount of melting in the mantle (James et al., 2010) and are important parameters in geodynamical modelling. Therefore, a thorough understanding of these parameters is necessary. However, few direct constraints can be placed on the thickness and density of the crust on Venus. For example, the lack of availability of seismic data because of the high surface temperature on Venus, results in the fact that there is no direct data available on the depth of the Moho.

One method for constraining the crustal thickness is the use of spectral measures that are sensitive to the topography and gravity. Examples of these spectral measures are the admittance and coherence. Because of the low resolution of the gravity data which is used for the calculation of the coherence, usually admittance data are used.

Anderson and Smrekar (2006) used admittance spectra to produce a high-resolution global admittance map of Venus. An inversion of this map resulted in estimates of the elastic, crustal and lithospheric thickness of Venus. The modelled ranges of crustal and elastic thickness were 0 – 90 km and 0 – 100 km respectively. The range in crustal thickness was interpreted by Anderson and Smrekar (2006) as an indication for Venus' present day activity.

Another method that is used to estimate the crustal thickness is based on the topography and gravity data while assuming isostatic compensation (see Section 3.1.3), but to date, few global maps of the crustal thickness of Venus have been produced (James et al., 2010). This is mainly due to the unconstrained Moho depth. However, according to James et al. (2010) even if a value for the average crustal thickness would be chosen, a global crustal thickness map of Venus is not easily produced. The main reason for this is that Venus' topography is probably supported by a number of sources, such as the isostatic compensation which results from variations in the thickness of the crust, lithospheric stresses, density anomalies in the crust and dynamic support in the form of dynamic topography (James et al., 2010).

James et al. (2010) were among the first to produce a global map of crustal thickness variations, by using Bouguer gravity anomalies in combination with the available detailed surface topography. James et al. (2010) found that the mean crustal thickness on Venus is approximately 30 km, which can be considered as an upper limit of the crustal thickness.

The mean crustal density was interpolated from measurements of gamma-ray backscattering by Venera 8 (Aitta, 2012) and was found to be approximately 2700 - 2900 kg m^{-3}.

4.2. The core

One of the first questions that was addressed concerning the core was whether the core is liquid, solid or has a solid inner core and a fluid outer core like Earth. As Venus appears to lack an internal magnetic field (Aitta, 2012) it seems plausible to assume that Venus has a different core structure than Earth in

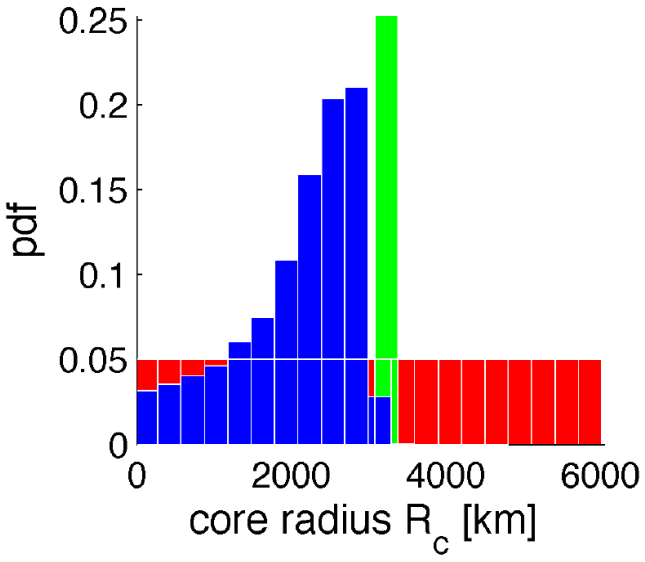

Figure 4: Figure from Dorn et al. (2014): the probability density function (pdf) of the core radius from an inversion method using mass and radius of Venus. The final, posterior estimate of the pdf (blue) calculated by inversion from a prior pdf estimate (red) is compared to an independent estimate of Aitta (2012) (green).

which at the least a growing solid inner core is absent. However, the lack of a magnetic field on Venus could also be explained by the slow spin rate of Venus or a lack of differentiation.

Evidence for a difference in core structure comes from the Doppler tracking data of the Magellan and Pioneer Venus Orbiter missions. From this, the second harmonic potential Love number k_2 has been estimated to be $k_2 = 0.295 \pm 0.066$ (Konopliv and Yoder, 1996). Modelling studies of the phase of the core and its Love number, predict a k_2 value of $0.23 \leq k_2 \leq 0.29$ for a liquid iron core and $k_2 = 0.17$ for a solidified iron core (Konopliv and Yoder, 1996). Hence, the Doppler data suggests that the core of Venus is liquid (Konopliv and Yoder, 1996). However, these estimates have been made while making assumptions on the viscosity of the core, which leads Bougher et al. (1997) to suggest that the fluidity of Venus' core is much like Earth's.

The second question concerning Venus' core relates to its size. Seismic data that could result in the determination of the core size are at present unobtainable, but the core size could also be determined from the moment of inertia factor of Venus, I/MR^2 (Mocquet et al., 2011). Here, I is the moment of inertia, M is the mass of Venus and R is the mean radius of Venus. The moment of inertia factor is a measure for the mass distribution in the planet. However, this values is at present unknown, because of the slow spin rate of Venus and its dense atmosphere which corrupts information due to the atmospheric drag on the spacecraft during measurements (Mocquet et al., 2011). Because of this, different methods are used to obtain first order constraints on the size of the core.

One of the most conservative models is to scale Earth's structure to the size of Venus and determine the core radius from this Yoder (1995). This results in a core radius of approximately

3000 km.

Aitta (2012) used a theoretical approach to calculate the size and composition of the core in which the mantle density is similar to that of Earth. It was found that the core is liquid with a radius of 3228 km and it has slightly more impurities than the inner core boundary fluid of the Earth (Aitta, 2012).

Dorn et al. (2014) used an inversion method based on Bayesian analysis to obtain a probability density function of the core radius from observations of the mass, radius and chemical composition of the planet. Dorn et al. (2014) found that the 95% credible interval of the core size is 0 to 2810 km (see Figure 4), which is slightly lower than the estimate by Aitta (2012). The reason for this is that Aitta (2012) found that the core is enriched in the lighter elements.

However, despite the various modelling and inversion studies, a definite estimate of the core size and composition of Venus is still unavailable. Therefore, a range of core sizes should be tested before conducting the actual parameter study. Yoder (1995), for example, tested core sizes ranging from 2700 km up to 3600 km to determine the most likely core size to conduct their studies with.

5. The thermal evolution of Venus

Now that the observations on the surface and the constraints on the interior of Venus have been presented, this information can be placed in the larger context of the thermal evolution of Venus. The present-day surface heat flux of Venus could provide some constraints on the thermal evolution of Venus, but at present no measurements of the surface heat flux have been made. Hence, other means of obtaining an estimate of the surface heat flux have been proposed. These methods typically stem from models and hypotheses on the thermal evolution of Venus. In the following, the most important thermal evolution models of Venus are discussed focusing on their prediction of the present-day heat flux. Besides that, the different global resurfacing models for the different thermal evolution models are discussed in terms of their ability to explain the observations. Lastly, the constraints that data can place on the nature and style of the global resurfacing event are discussed.

5.1. Uniformitarian model

In the uniformitarian model there is a balance between the radiogenic heat and heat from the secular cooling on the one hand and the heat transport through the mantle and the lithosphere on the other hand (Schubert et al., 2001). This balance is maintained through a thin, stable lithosphere in which heat is transported by conduction. For this near-steady-state heat loss model, the surface heat flux can be obtained by scaling the Earth's heat loss to Venus according to the mass ratio between the two planets (Turcotte, 1995):

$$q_{s,V} = \frac{M_V}{M_E} \cdot \frac{Q_E}{4\pi R_E^2}, \tag{2}$$

where the subscript E and V denote Earth and Venus respectively. Using $M_V = 4.87 \times 10^{24}$ kg, $M_E = 5.97 \times 10^{24}$ kg and $R_E = 6371 \times 10^3$ m, Turcotte (1995) found a surface heat flux of $q_{s,V} = 63$ mW m^{-2}, when they use a heat flux of $Q_E = 3.55 \times 10^{13}$ W for Earth. Using the same method, but another value for the heat flux of Earth $Q_E = 4.2 \times 10^{13}$ W, Solomon and Head (1982) found a surface heat flux of $q_{s,V} = 74$ mW m^{-2}. The difference in these estimates arises from a different assumption on the Earth's heat flux. Therefore, there is a large uncertainty in these estimates even for one specific model. The estimate of the Venusian heat flux that is the most generally accepted is $q_{s,V} = 74$ mW m^{-2} and other models (see Sections 5.2 and 5.3 for example) try to fit this estimate using, for example, heat fluxes that vary over time.

The scaling of the two planets implicitly assumes that the amount of heat-producing elements is similar in both Venus and Earth. This assumption is reasonable and in accordance with the present-day understanding of planetary accretion (Schubert et al., 2001). Considering the similar size between Earth and Venus, it is also likely that the heat from secular cooling is similar. As Venus does not display plate tectonics as on Earth, another mechanism for heat transport is necessary for the uniformitarian hypothesis. This mechanism could be the transport of larger material fluxes through the mantle, which leads to a more vigorously convecting mantle and a higher Rayleigh number. As the Rayleigh number is most sensitive of the viscosity of the mantle (see Section 9.1 for the definition of the Rayleigh number), this implies that the mantle of Venus has a smaller viscosity than Earth, when the uniformitarian model is considered.

5.1.1. The equilibrium volcanic resurfacing hypothesis

The equilibrium volcanic resurfacing hypothesis aims to explain Venus' surface features through continuous volcanic and tectonic activity, and is in line with the uniformitarian thermal evolution model of Venus. This hypotheses is able to explain the near-random impact crater distribution and the global surface age of Venus. If there was near-continuous volcanic and tectonic activity, one would expect a lot of impact craters to be (at least partially) buried by volcanic flows. This is in line with the interpretation of the data by Herrick and Rumpf (2011), but Hansen and Young (2007) argued that this hypothesis is unlikely, because of their interpretation of the data as pristine impact craters on the surface of Venus (see Section 3.3.2).

If a global resurfacing event is assumed, the volcanic activity should have been able to bury impact craters older than ~500 Myr. As the heights of impact crater rims can be up to 650 m (see Section 3.3.2), global lava flow stacks of over 750 m thick would be required (Hansen and Young, 2007). Although thick lava flows could accumulate to this thickness over time, the analysis of SAR images show the presence of extensive thin lava flows on Venus (see Section 3.3.2).

Hence, the equilibrium volcanic resurfacing hypothesis is able to explain some of the geological observations, but fails to explain others. To which extent the equilibrium resurfacing hypothesis is plausible, depends on which of the different interpretations of impact crater data is favoured.

5.2. Catastrophic model

In accordance with the observations that lead to the proposal of a resurfacing event, the catastrophic model explains the heat loss of Venus through a series of global subduction episodes of the lithosphere (Schubert et al., 2001). It is assumed that the lithosphere stabilized itself around 500 Myr ago after the last global resurfacing event. Since then, the interior of the planet has been heating up.

Several alternative models have been proposed to explain Venus' thermal evolution of the last 500 Myr, which are discussed in this section.

5.2.1. Global overturn followed by surface quiescence

Arkani-Hamed and Toksöz (1984) and Arkani-Hamed (1994) suggested that the mantle of Venus was very convective until 500 Myr ago, which resulted in the solidification of the core of Venus. In the last 500 Myr the plate tectonics on Venus ceased and a buoyant crustal lid formed on Venus, which resulted in the present-day hot spot volcanism as a means of cooling the planet. Hence, Arkani-Hamed and Toksöz (1984) and Arkani-Hamed (1994) proposed that the last global resurfacing event 500 Myr ago is (and will be) followed by surface quiescence.

As discussed in section 4.2, the prediction of the solid core is not yet supported by data. In contrast, the data suggest a completely liquid core or an Earth-like core which has partly solidified. Besides that, the estimated heat production in the interior of Venus is not in balance with the estimated surface heat flux which results from hot spot volcanism and conduction through the buoyant crustal lid.

5.2.2. The episodic global subduction hypothesis

Turcotte (1993) and Turcotte (1995) stated that the internal temperature build up in Venus will ultimately trigger another global subduction event in the future (after the most recent global overturn of the mantle), as the thickened lithosphere will become unstable eventually. Another mechanism for the periodic overturn of the mantle could be that the mantle convection is periodic due to chemical differentiation (see Schubert et al. (2001) and references therein).

Based on the half-space cooling model, a prediction of the present-day surface heat flux can be made for both catastrophic models with the following equation (Turcotte, 1993):

$$q_s = \frac{k(T_m - T_s)}{\sqrt{\pi \kappa t}}, \tag{3}$$

where $k = 3.3$ W m^{-1} is the thermal conductivity, $T_m = 1500$ K is the mantle temperature, $T_s = 750$ K is the surface temperature, $\kappa = 1 \times 10^{-6}$ m^2 s^{-1} is the thermal diffusivity, and $t = 500$ Myr is the time. This results in a present-day surface heat flux of $q_s = 11.1$ mW m^{-2}. This is significantly lower than the estimated surface heat flux from the Earth scaling. To account for the remaining heat removal, Turcotte (1993) suggested a vigorous episode of tectonics and volcanism after a global resurfacing event, but before surface quiescence. However, Ghail (2015) pointed out two main problems with this hypothesis. First, the global resurfacing event is the process that stabilises the lithosphere, by generating new lithosphere. Besides that, the vigorous process that was proposed cannot be tested numerically or geologically.

5.2.3. The catastrophic volcanic resurfacing hypothesis

The resurfacing event proposed by the catastrophic volcanic resurfacing hypothesis consists of the geologically rapid (10 - 100 Myr) burial of preexisting impact craters by means of lava flows with a thickness of 1 - 3 km across Venus's surface (Hansen and Young, 2007). This way, the current near-random distribution of impact craters can be explained by the initial craterless surface that would be a result of the burial of preexisting craters.

However, not all the observations can be explained by the catastrophic volcanic resurfacing hypothesis. For example, observations show that Venus is mostly covered in thin lava flows (see Section 3.3.2) instead of the thick lava flows proposed by this hypothesis. Besides that, the distinct regions of different average surface age are not explained by this hypothesis, because all impact craters would have been buried at approximately the same time, leading to a uniform global surface age (Hansen and Young, 2007). In order to overcome this problem of different average surface ages, slight variations of the catastrophic volcanic resurfacing hypothesis can be proposed. For example, three stages of volcanic burial could account for the different surface ages.

5.2.4. The global stratigraphy model

The global stratigraphy model is a stratigraphic model consistent with the catastrophic volcanic resurfacing hypothesis. It states that before the mean surface age t there was global deformation of tesserae, followed by several stages of extensive volcanism (Basilevsky and Head, 1998). During this stage, parts of the tesserae were buried and the regional plains were formed (Basilevsky and Head, 1998). Next, successive episodes of compression, tension, compression and finally, tension characterized the history of Venus. This series of tectonic deformation was derived from the unconformities visible in photos and radar images from the surface of Venus which showed tesserae, dense fractioning, broad ridging and wrinkle ridging (Basilevsky and Head, 1998). At time t until the present, Venus tectonic history was mainly characterized by regional rifting and volcanism related to that.

According to Hansen and Young (2007) this global stratigraphy model could predict regions of different surface age, due to the episodes of compression and tension. The higher-lying crustal plateaus could be associated with a higher surface age, while the lowlands could be associated with a lower surface age, as a result of volcanic flooding. However, this is in direct contrast with the interpretation of the data by Hansen and Young (2007) (see Section 3.3.2). However, as the global stratigraphy model is a model inferred from the observations that the plains are younger than the tesserae and the rifts and volcanoes are younger still, the argument from Hansen and Young (2007) is

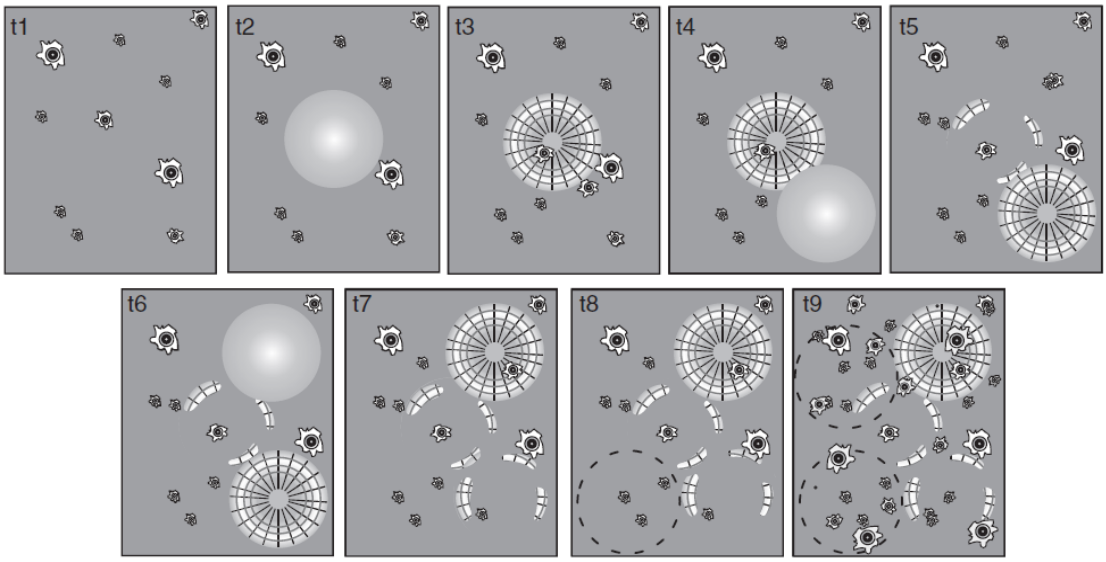

Figure 5: Figure modified from Hansen and Young (2007). Time evolution of the surface of Venus as predicted by the SPITTER stratigraphic model. The various stages of the evolution are described in the text.

likely incorrect. The global stratigraphy model proposes thick lava flows like the catastrophic volcanic resurfacing hypothesis, while observations indicate thin lava flows. The observation of thin lava flows could however be just a regional observation. Whether or not the global resurfacing event was accommodated by thick lava flows is one the predictions that future missions to Venus could test.

5.2.5. The SPITTER model

The SPITTER model is a stratigraphic model that is consistent with the catastrophic evolution model and was recently developed by Hansen and Young (2007). The SPITTER-hypothesis, short for Spatially Isolated Time-Transgressive Equilibrium Resurfacing hypothesis, proposes an evolution of Venus' surface in various stages (see Figure 5 for a graphic evolution of the surface of Venus according to the SPITTER model): *(i)* Initially meteorites impacted the surface of Venus and Venus had a thin lithosphere (stage t1 in Figure 5). *(ii)* Next, a crustal plateau with characteristic tessera was formed on this lithosphere, thereby effectively destroying the impact craters within the plateau (stages t2 and t3 in Figure 5). *(iii)* After this, a new crustal plateaus formed, which again destroyed impact craters in its area. At the same time, the first crustal plateau could decay topographically, while leaving the tessera intact. Thin volcanic flows could in turn bury parts of the tessera, but are too thin to completely cover the impact craters (stages t4 and t5 in Figure 5). *(iv)* Continuing this sequence results in the destruction of impact craters by the formation of crustal plateaus and the covering of the surface in various layers of thin lava flows (stages t6 and t7 in Figure 5). At the same time volcanic rises could develop on top of mantle plumes, as indicated in stage t8 in Figure 5 by the dashed circle. *(v)* Over time, the whole lithosphere of Venus is thickened by these processes. When a sufficiently thick lithosphere is reached, the crustal plateaus that were formed just prior to this are preserved (stage t9 in Figure 5).

The main difference between the SPITTER model and the global stratigraphy model is that the SPITTER model states that the stratigraphic sequence is a result of regional tectonics instead of global tectonics. The SPITTER hypothesis can explain a lot of the observations that were interpreted by Hansen and Young (2007). For example, the SPITTER-hypothesis proposes that the lowland regions could be remnants of ancient crustal plateaus. Hence, the SPITTER-hypothesis is able to explain the correlation between the old average surface age and the lowland regions.

However, the main problem with both the global stratigraphy model and the SPITTER model is that they treat the radar images as photographs, which could lead to the erronous interpretation of some stratigraphic units.

5.3. Differentiated planet model

The differentiated planet model assumes that the heat-producing elements are not equally distributed in the planet's interior (like the uniformitarian model), but are instead fractionated into the crust. The generated heat is then lost through conduction. Schubert et al. (2001) showed that it is possible to construct a differentiated model in which the mantle is solid if almost all the heat-producing elements are located in the crust, there is little to no secular cooling of Venus, and the heat-producing elements are located uniformly through the crust.

The assumptions that all the heat-producing elements are situated in the crust and that there is no secular cooling simplifies the model for the surface heat flux even more. The surface heat flux is then given by the following equation:

$$q_s = \rho_c H_c y_c \tag{4}$$

where $\rho_c = 2900$ kg m^{-3} is the crustal density, H_c is the heat production and y_c is the thickness of the crust. This equation

can be solved if the heat production and thickness of the crust are known. Estimates for these values are determined by Schubert et al. (2001) for different values of the Urey ratio. The Urey ratio U is the ratio between radiogenic heat production H and the total surface heat flux q_s of the planet:

$$U = \frac{H}{q_s} \tag{5}$$

The remaining heat is supplied by the secular cooling of the planet. For an Urey ratio of 0.6 Schubert et al. (2001) found $H_c = 130 \times 10^{-12}$ W kg^{-1} and $y_c = 100$ km, which results in a surface heat flux of $q_s = 37.7$ mW m^{-2}. An Urey ratio of 0.8 results in $H_c = 230 \times 10^{-12}$ W kg^{-1} and $y_c = 75$ km and a subsequent surface heat flux of $q_s = 50.0$ mW m^{-2}.

The implication of this model is that most likely the crust would have thickened over time while there is also very little crustal recycling. This could then result in depletion of the mantle of radiogenic elements, which could lead to a reduction of radiogenic elements in volcanic surface rocks and a decay in the amount of volcanism over time.

5.4. Subcrustal lid rejuvenation model

The subcrustal lid rejuvenation model is an alternative hypothesis that was recently proposed by Ghail (2015). It is based on a possible decoupling between the crust and mantle part of the stagnant lid, assuming that Venus is at present in a stagnant lid regime. The stagnant lid regime is a regime in which a rigid, stagnant lid overlies a convecting mantle (see also Section 6). Ghail (2015) showed that Venus' crust is partly decoupled from the mantle for typical geological strain rate of $\sim 10^{-15}$ s^{-1} for various temperature gradients. A detachment layer forms when the thickness of the crust ranges from 10 - 15 km. If the mantle part of the stagnant lid is sufficiently detached from the crust, this lid can be rejuvenated by thinning and subsequent recycling, which would be a subcrustal analogue to the surface plate tectonics on Earth.

A simple cooling half-space model with an upper boundary condition of the temperature at the bottom of the crustal layer T_c was used to estimate the heat flux predicted by this model. A surface heat flux of 71.2 mW m^{-2} was found for a lid recycling rate of 4.0 ± 0.5 km^2 yr^{-1} (Ghail, 2015). Assuming that the present-day surface heat flux of Venus should be 74 mW m^{-2} based on the scaling from Earth to Venus, there is a $\sim 10\%$ deficiency in the surface heat flux of the subcrustal lid rejuvenation model. This deficiency can be explained by radiogenic elements in the crust, which were not taken into account in this simple calculation and by heat loss from the core (Ghail, 2015). The implication of these results is that Venus is able to maintain a stable tectonic regime without episodic global resurfacing by means of rejuvenating the subcrustal lid.

Two possible mechanisms for the lid rejuvenation have been proposed. The first mechanism is lid rejuvenation by plumes. When a mantle plume impinges on a stagnant lid, the lid will become warmer and thinner and is uplifted as a result. At the surface of Venus this would be displayed as a large topographic swell. Nine topographic swells with diameters of ~ 1000 km that could possibly be the result of plume impinging have been identified on Venus. In order to lose the amount of heat that was estimated for Venus by the scaling from Earth, approximately 75 ± 2 plumes similar to the Hawaiian plume in size should be active at any time on Venus. This is more than ten times the amount of active topographic swells that is estimated for Venus at present (Ghail, 2015).

The second mechanism is delamination of the subcrustal lid, which can occur when the crustal detachment layer is sufficiently weak.

Although the crust is detached from the mantle in this model, the crust moves vertically because of the cooling and heating of the subcrustal lid beneath it. Observations show an association between topographic rises and rifts and other features, which could indicate that subcrustal lid rejuvenation drives geological processes at present (Ghail, 2015).

5.5. Constraints from data

Apart from the theoretical hypotheses for the global resurfacing event, statistical analysis of the impact crater observations is another method that is used to determine Venus' tectonic surface evolution.

In an early study, Bullock et al. (1993) used a 3D Monte Carlo model of the resurfacing event in which the observed distribution of volcanic features from the Magellan mission was incorporated. Assuming that the impactor and volcanism rates were constant, the following scenario of the resurfacing event resulted in surfaces statistically equivalent to that of Venus: a volcanic flux of 0.37 km^3 yr^{-1} operating for 550 Myr on a surface that was initially craterless.

Strom et al. (1994) used Monte Carlo simulations as well to estimate that only 4% - 6% of Venus' surface has been volcanically resurfaced after the global resurfacing event around 300 Myr ago which yielded a near craterless surface. Similarly, Price and Suppe (1995) concluded that about 14% of Venus has been resurfaced by volcanism in addition to the 6% that has been resurfaced by tectonic deformation, by studying the hypsometry and the distribution of volcanism and impact craters. The lava production rate in the period after resurfacing was 0.01 - 0.15 km^3 yr^{-1} according to Strom et al. (1994), with most of the recent volcanism on Venus occurring in the Beta-Atla-Themis region.

By studying the impact crater densities on coronae and large volcanoes, Namiki and Solomon (1994) also concluded that volcanoes and volcanism associated to coronae have been active for the last 500 Myrs on Venus.

More recently, Romeo (2013) investigated four different resurfacing models using Monte Carlo statistics on the interaction between inpact cratering and volcanism. The main aim of this study was to explain the observations in the Beta-Atla-Thermis region. The first two models were catastrophic resurfacing models, with one model having a drastic decay of volcanic activity after the resurfacing event and the other model having only a moderate decay. The third and fourth models

were both equilibrium resurfacing models, with one model having a magmatic event followed by gradual decay of volcanism. The other model was similar, but lacked the magmatic event. The model that best explained the observations of the Beta-Atla-Thermis region is the first model of global catastrophic resurfacing followed by drastic decay of the volcanic activity.

In an attempt to explain the presence of both young and old volcanic plains, Ivanov and Head (2014) investigated the proportion of impact craters in these features in order to estimate the size of the volcanic resurfacing event. It was found that the style of volcanic resurfacing on Venus has changed during the last 500 Myr: at first there was global volcanic activity, which resulted in the formation of regional plains. After this stage, the volcanism became more localized.

O'Rourke et al. (2014) used Monte Carlo simulation to distinguish between two possible styles of volcanic resurfacing: thin lava flows or large shield volcanoes. The impact crater distribution on Venus is best explained by a model with localized thin lava flows according to O'Rourke et al. (2014).

The results from the studies mentioned above are all inconsistent with pure catastrophic or equilibrium models for the global resurfacing event. Instead, these studies indicate that the resurfacing event was a more complex event. The range in conclusions between these models stems from the fact that these studies are based on simplistic assumptions concerning the style of the global resurfacing event, so the results most probably fail to capture the full complexity of the resurfacing event.

Herrick (1994) summarized the resurfacing history of Venus by distinguishing the following stages in the history of Venus: *(i)* Before 800 Ma the crust of Venus was tectonically deformed because of horizontal movement. *(ii)* Then, 800 - 300 Myr ago, a global resurfacing event in the form of a brief period of global volcanism resulted in a nearly uniform elevation accross the planet. *(iii)* After the global resurfacing event, the geology of Venus has been dominated by large volcanoes and limited horizontal movement of the crust. The cause that Herrick (1994) proposed for this geologic history is the cooling of the mantle which caused the lithosphere to become positively buoyant.

The models that are discussed here each provide an explanation for the thermal evolution of Venus. If future missions to Venus could measure the surface heat flux on Venus, a preferred model can be chosen. This model should also be able to explain the global resurfacing event $\sim$ 500 Myr ago. The model that is most designed to fit this specific part of Venus' history is the catastrophic model.

6. Previous modelling studies

Numerical models are used to test the various hypotheses on Venus in a self consistent manner. The main focus of models focusing on the recent mantle evolution of Venus has been to test the conditions under which Venus is in the stagnant regime, periodic regime or the mobile lid regime. The stagnant lid regime is the presumed present-day regime of Venus, which supports the uniformitarian model (Section 5.1), the catastrophic model in which the global resurfacing event is followed by surface quiescence (Section 5.2.1) and the differentiated planet model. The periodic regime predicts episodes of global mantle overturn, consistent with the catastrophic model (Section 5.2.2). The mobile lid regime is the present-day regime of Earth, and there is little indication that Venus is in the mobile lid regime at present, but Venus could have been in the mobile lid regime in the past.

In order to study the thermal evolution models of Venus that have been discussed in Section 5, ideally three dimensional models of Venus are run from the formation of Venus up until present. This is however, computationally too demanding and therefore, at present, not realistic. However, the use of the parameterized convection approach ensures that the thermal evolution models can be studied numerically. This method uses the Nusselt number - Rayleigh number relation to account for the contribution of mantle convective heat transfer to the overall energy balance of a planet. Numerous studies using the parameterized convection models have been conducted, but these are not discussed here, because the modelling study of this work focuses on a model with dimensions (see Section 7). Instead, other numerical models are discussed which are not necessarily based on the parameterized convection approach.

One of the earlier, simple models of the mantle convection on Venus with a constant viscosity and lacking any phase changes, was studied by Schubert et al. (1990). The three dimensional spherical models were heated from below and internally. The upper boundary represented the base of a rigid, isothermal lithosphere or was stress-free, in order to assess the role of the rigid lithosphere on the mantle convective regime. The mantle thickness was assumed to be 2941.5 km, in accordance with an assumed core size of 3110 km. This estimation of the mantle thickness resulted from an assumed ratio $R_{inner}/R_{outer} = 0.514$, where R_{outer} is the radius of Venus and R_{inner} is the radius of the core of Venus, based on the assumption that Venus' mantle is probably slightly thicker than Earth's mantle (Schubert et al., 1990). It was found that models with a rigid lithosphere as upper boundary have a higher surface and mantle temperature and there were more upwellings than models with a stress-free boundary condition. The mantle convective regime with a rigid lithosphere was overall characterized by closely spaced, short wavelength features. Schubert et al. (1990) suggested that the mantle plume activity could cause the clustering of coronae on Venus.

After initially simple models, such as the one described above, a range of parameters was investigated to quantify their influence on the mantle convective regime on Venus. In this section, the influence of phase changes and viscosity on the mantle convective regime are discussed. Lastly, the models that incorporate complex rheologies in order to better capture the whole mechanics of Venus' mantle convection are discussed.

6.1. *Influence of viscosity*

Several studies regarding the influence of the viscosity of the mantle convective regime on Venus have been conducted. Usually a simple temperature-dependent viscosity implementation

is used to describe the rheology of Venus' mantle (Schubert et al., 2001). For numerical calculations of the Earth, such a simple implementation would be insufficient and a more complex rheology is needed to describe the brittle and ductile failures that accompany Earth's plate tectonic regime. However, as Venus does not display plate tectonics, this simple approach is sufficient (Schubert et al., 2001). A temperature-dependent viscosity easily results is a stagnant lid regime if the viscosity contrast is big enough. Therefore, one of the most distinct effects of the viscosity is that it determines in which mantle convective regime Venus is.

To illustrate and quantify this, Schubert et al. (2001) conducted a series of models with different viscosity contrasts. Each model was a $8 \times 8 \times 1$ rectangular box with free slip and isothermal top and bottom boundary conditions and periodic side boundaries. It was found that low viscosity contrasts of $1 - 10$ are characterized by a fairly symmetrical spoke pattern of up- and downwellings (Schubert et al., 2001). For slightly higher viscosity contrasts of $10^2 - 10^3$ the model results are characterized by an asymmetric long wavelength pattern of a cylindrical downwelling surrounded by narrow upwellings. High viscosity contrasts of $10^4 - 10^5$ result in a small wavelength pattern of upwellings and downwellings under a stagnant lid. The increase of the viscosity contrast results in a lower Nusselt number and an increasing velocity. These findings are supported by theory (Solomatov, 1995) and spherical three dimensional models (see Schubert et al. (2001) and references therein).

Trompert and Hansen (1998) used a more complex rheology that is both temperature and strain rate dependent combined with the concept of a yield stress:

$$\mu = \frac{2}{\frac{1}{\mu_T} + \frac{1}{\mu_\varepsilon}} \tag{6}$$

with

$$\mu_T = \exp(-RT), \tag{7}$$

and

$$\mu_\varepsilon = \mu^* + \frac{\sigma}{\sqrt{\dot{\boldsymbol{\varepsilon}} : \dot{\boldsymbol{\varepsilon}}}}, \tag{8}$$

where R is a constant that controls the viscosity contrast due to temperature, μ^* is the effective viscosity at high stresses, σ is the yield stress, and $\dot{\boldsymbol{\varepsilon}}$ is the strain rate tensor. The use of this rheology results in a rigid lid on top of a convective fluid, that can break if the stresses are high enough (Trompert and Hansen, 1998). The model that was considered was a Cartesian box of $4 \times 4 \times 1$, with a heated bottom. Assuming that the height of the box is equal to the depth of the mantle, a domain of $11600 \times 11600 \times 2900$ km was modelled (Trompert and Hansen, 1998). The model resulted in periodic regimes with episodes of subduction and growth of a stagnant lid. The duration of the mantle overturns can be roughly estimated by dimensionalizing the time between overturns (~ 0.04) according to the following relation:

$$t = t' \cdot \frac{D^2}{\kappa} \tag{9}$$

where t is the time in seconds, t' is the dimensionless time, $D = 2900$ km is the reference length and κ is the thermal diffusivity. For simplicity, the thermal diffusivity is assumed to be 10^{-6} m^2 s^{-1}. The duration of the period of mantle overturn then can be calculated to be approximately 10660 Myr. This period of overturn is too large, taking into consideration that Venus is only 4600 Myr old. However, the reason for this could be the simplicity of the model, as the model lacks, for example, phase boundaries, internal heating and continents.

6.2. *Influence of phase changes*

Phase changes are important parameters for studying the mantle convection of Venus, because they have the potential to stratify the mantle convection. One of the first studies to investigate the influence of phase changes on the style of convection of Venus was conducted by Steinbach and Yuen (1992). The tested models were two dimensional boxes with an aspect ratio of four. Models with both an olivine → spinel phase change and a spinel → perovskite phase change favoured layered mantle convection, while a model with only the spinel → perovskite model did not favour the layered mantle convection as strongly. The different phase transition depth in Venus compared to Earth, increased the tendency towards whole mantle convection. This convection regime is also favoured by a potentially lower Rayleigh number in Venus. Steinbach and Yuen (1992) speculated that a change in the style of convection regime from layered in the past to whole mantle convection at present may have been responsible for the global resurfacing event 500 Myr ago. This is then in line with models predicting only a single global resurfacing event in the history of Venus.

Three dimensional models with phase changes were conducted by Schubert et al. (2001) and included the exothermic phase change at a depth of 440 km and an endothermic phase change at a depth of 740 km. The spherical models had isothermal boundary conditions and an inner boundary condition of free slip, and a rigid outer boundary. The viscosity is dependent on the density via a power-law. The results showed a convective style similar to that of Earth models: the upper mantle contains downwellings that cannot initially break the layering which results from the phase change so that cold material accumulates at this discontinuity. When enough cold material is accumulated the material breaks through the discontinuity into the lower mantle. As the timing of breakthroughs at different locations in the model overlap, the mantle is never fully in the layered mantle convection regime or the whole mantle convection regime. A quick comparison to previous models without a phase change, as discussed in Section 6 show that the models that include phase changes are characterized by longer wavelength features.

6.3. *Influence of phase changes together with viscosity*

A first step towards a more complex model of Venus' mantle consisted of implementing both phase changes and viscosity

simultaneously in a $4 \times 4 \times 1$ model in order to study their combined effect on mantle convection (Schubert et al., 2001). The box was heated from below and had isothermal bottom and top boundary conditions. The side boundaries were reflecting boundaries. The phase changes at 440 km and 740 km were included and three different viscosity implementations were tested: *(1)* The model with a constant viscosity shows weakly time-dependent, whole mantle convection in which broad up- and downwellings easily penetrate the phase changes. The mode of convection is similar to models without phase changes (Schubert et al., 2001). *(2)* The model with a variable viscosity shows some degree of layering in which the broad, sheet-like downwellings cannot penetrate the phase transition, but smaller features such as cold plumes are able to get into the lower mantle. Like the constant viscosity mantle, this model is weakly time-dependent. *(3)* The model with a variable viscosity with a yield stress shows a very strong time dependence with heat fluxes varying from 20 to 45 mW m^{-2}. The most dominant features are subduction-like, linear zones of downwellings. This model most accurately predicts the episodic global subduction hypothesis, as discussed in Section 5.2.2. The degree of layered mantle convection varies in this model, because of the periodic character of the mantle convection. It was concluded that the inclusion of a temperature-dependent viscosity favours layered mantle convection (Schubert et al., 2001). Case *(2)* would most likely represent Venus, as Venus does not display plate tectonics (case *(3)*). This would implicate that Venus' mantle convective regime is at present layered.

6.4. Advanced models

Apart from modelling studies that investigate the influence of various parameters on the mantle convective regime on Venus, several recent studies have endeavored to capture the complexity of Venus' mantle convection. In this section several studies that aim to explain some of Venus' features are briefly discussed.

An advanced, numerical, spherical, two dimensional mantle convection model that focused on capturing the complex processes in the mantle of Venus was conducted by Armann and Tackley (2012). The model included melting, magmatism, internal heat production, cooling of the core and a temperature-dependent viscosity and was compared to the topography and geoid observations (Armann and Tackley, 2012). Both stagnant lid and episodic lithospheric overturn models were run. It was found that the stagnant lid convection requires massive magmatism to accommodate heat loss in a magmatic heat pipe as its dominant mode of heat loss. This massive magmatism would lead to a very thick crust, which is inconsistent with the observations. The episodic models predict $5 - 8$ overturns during the entire evolution of Venus' history, which each last for approximately 150 Myr. An episode of global overturn typically initiates at one location, after which it spreads globally. Both types of models, stagnant and episodic lid, are capable of producing a topography and geoid that resemble the observations on Venus.

In a follow-up study, Gillmann and Tackley (2014) studied the coupling and feedbacks between the mantle and the atmosphere on Venus. More specifically, the degassing of the mantle and of atmospheric escape into space were coupled and studied to obtain a model of coupled mantle and atmosphere evolution. Episodic overturns replenish the atmosphere over time by means of volcanic degassing. It was found that the CO_2 pressure is relatively stable over time, but the atmospheric water vapor pressure is sensitive to volcanic activity, which can lead to changes in the surface temperature of up to 200 K. This prediction from modelling could be used during future space missions to Venus as an additional possible means of detecting active volcanism on Venus. When there is a low surface temperature, a mobile lid regime is triggered. Otherwise a stagnant lid regime is dominant.

Besides whole mantle convection studies, advanced models regarding specific surface features of Venus have also been conducted. An example of these, is the first three dimensional model of the formation and evolution of coronae on Venus by Gerya (2014). In this study, a mantle plume was modelled that impinged warm, thin lithosphere in order to obtain a corona-like structure. The numerical results suggests that coronae can form from magma-assisted convection of ductile, weak crust which results from the decompression melting of a rising mantle plume. In the first stage of the formation of a corona, a topographic rise is formed, after which it dips inwards causing fracturing and thrusting.

It is clear that the mantle convection of Venus has already been studied rigorously in detail, but a lot of work still remains to be done. One of the major flaws of the previously described models is that they assume a mantle thickness and core-mantle boundary temperature at the start of their modelling study and then focus on the effects of other parameters, such as viscosity, without first assessing the role of the mantle thickness and the core-mantle boundary temperature. It is particularly important to look at the effect of these two parameters, because they are poorly constrained. Furthermore, the models described above all either use a constant thermal conductivity k or a pressure (or depth) dependent conductivity. However, Hofmeister (1999) and van den Berg et al. (2001) proposed a temperature and pressure-dependent conductivity. The effect of this conductivity has not yet been tested on mantle convection models of Venus. Lastly, the recently proposed hypothesis of subcrustal lid rejuvenation has not been tested numerically yet. Therefore, a new modelling study is proposed in which these issues are addressed.

7. Modelling approach

The modelling study conducted in this work aims to shed more light on the conditions under which the different mantle convective regimes are stable, taking into account the different possibilities of the mantle thickness (see also Section 4.2) and temperature of the core-mantle boundary. More specifically it is investigated when the mobile lid, periodic and stagnant lid regime are stable with respect to the yield stress of the lithosphere. Besides that, the influence of a temperature- and

pressure-dependent thermal conductivity on the mantle convection regimes is investigated. The recently proposed subcrustal lid rejuvenation model by Ghail (2015) is also briefly investigated. In this section the code ASPECT that was used and the model setup are described.

7.1. ASPECT

For the modelling study the massively parallel code ASPECT (Advanced Solver for Problems in Earths ConvecTion) (Kronbichler et al., 2012) for (in)compressible flows is used. ASPECT is a finite element code with second order elements, which uses the numerical software packages DEAL.II[2], TRILINOS[3], P4EST[4] and an iterative solver. Key features of ASPECT include its flexibility with regards to geometries, as two and three dimensional Cartesian, cylindrical and spherical geometries are implemented; the implementation of a viscoplastic rheology and an adaptive mesh refinement scheme (Kronbichler et al., 2012).

ASPECT is capable of solving the compressible Stokes flow equations and the complete heat equation, but for this modelling study the following equations were used (see Table 5 for an explanation of the symbols used in the equations):

$$\boldsymbol{\nabla} P - \boldsymbol{\nabla} \cdot (2\mu\dot{\boldsymbol{\varepsilon}}) = \rho \boldsymbol{g}, \tag{10}$$

$$\boldsymbol{\nabla} \cdot \boldsymbol{u} = 0, \tag{11}$$

$$\rho C_p \Big(\frac{\partial T}{\partial t} + \boldsymbol{u} \cdot \nabla T \Big) - \nabla \cdot k \nabla T = 0 \tag{12}$$

Here, equation (10) is the momentum conservation equation, equation (11) is the incompressibility constraint from the mass conservation equation, and equation (12) is the heat equation. In this system of equations, the velocity and pressure are dependent on both time t and position $\boldsymbol{x}$. For a more detailed analysis of the equations and implementations of various features in ASPECT, the reader is referred to Kronbichler et al. (2012) and Bangerth et al. (2015).

7.2. Model setup

As a model setup a dimensionalized version of the viscoplastic thermal convection benchmark from Tosi et al. (2015) is used. The domain is a two-dimensional square box of dimensions $D \times D$ (see Figure 6), where D is the thickness of the mantle. The gravity acceleration[5] in the model g is 8.87 m s^{-2}, as on Venus. Constant material properties in the model, are the density ρ = 3300 kg m^{-3} and the heat capacity C_p = 1060 J kg^{-1} K^{-1} (see also Figure 6). The value for the heat capacity results from the constant value for the density, the thermal diffusivity (10^{-6} m^2 s^{-1}) and the surface thermal conductivity (3.5 W m^{-1} K^{-1}) by using the following equation (see Table 5 for an explanation of the used symbols):

$$C_p = \frac{k}{\rho \kappa} \tag{13}$$

The mechanical boundary conditions are free slip conditions on all boundaries, so that $\tau_{xy} = \tau_{yx} = 0$ and $\boldsymbol{u} \cdot \boldsymbol{n} = 0$. The temperature and pressure boundary conditions at the top of the domain are a surface temperature T_s = 740 K and a surface pressure P = 9.3 MPa for the standard models (see Section 2 and Table 2). To investigate the subcrustal lid rejuvenation hypothesis of Ghail (2015), the top boundary conditions are changed to a surface temperature T_s = 900 K and a surface pressure P = 300 MPa. These values correspond to the values at the base of the crustal layer in the subcrustal lid rejuvenation model. The temperature boundary condition at the bottom of the domain is a fixed core-mantle boundary temperature T_{cmb}. As the mantle thickness D and the temperature at the core-mantle boundary T_{cmb} are still largely unconstrained (see Section 4) both quantities are varied to investigate their influence on mantle convective regimes. As temperature boundary

Table 5: Nomenclature

Symbol	Parameter	Unit
$\mathbf{1}$	Unit matrix	-
α	Thermal expansion coefficient	K^{-1}
γ	Grueneisen parameter	-
γ_T	Viscosity contrast due to temperature	Pa s
γ_y	Viscosity contrast due to depth	Pa s
κ	Thermal diffusivity	m^2 s^{-1}
$\Delta\mu_T$	Viscosity contrast due to temperature	Pa s
$\Delta\mu_y$	Viscosity contrast due to depth	Pa s
$\dot{\boldsymbol{\varepsilon}}, \dot{\varepsilon}_{ij}$	Strain rate	s^{-1}
μ	Viscosity	Pa s
μ^*	Effective viscosity at high stresses	Pa s
μ_{lin}	Linear viscosity	Pa s
μ_{plast}	Non-linear, plastic viscosity	Pa s
ρ	Density	kg m^{-3}
σ_Y	Yield stress	Pa
τ_{xy}, τ_{yx}	Shear stress	Pa
a	Fitting parameter	-
D	Thickness of the mantle	m
C_p	Specific heat capacity	J kg^{-1} K^{-1}
$\boldsymbol{g}$	Gravity acceleration	m s^{-2}
k	Thermal conductivity	W m^{-1} K^{-1}
k_0	Reference thermal conductivity	W m^{-1} K^{-1}
K_0	Bulk modulus	Pa
K_0'	Pressure derivative bulk modulus	-
P	Pressure	Pa
t	Time	s
T	Temperature	K
T_{cmb}	Core-mantle boundary temperature	K
T_s	Surface temperature	K
$\boldsymbol{u}, u_x, u_y$	Velocity	m s^{-1}

[2] https://www.dealii.org
[3] http://trilinos.org
[4] http://www.p4est.org
[5] https://solarsystem.nasa.gov/planets/profile.cfm?Object=Venus&Display=Facts

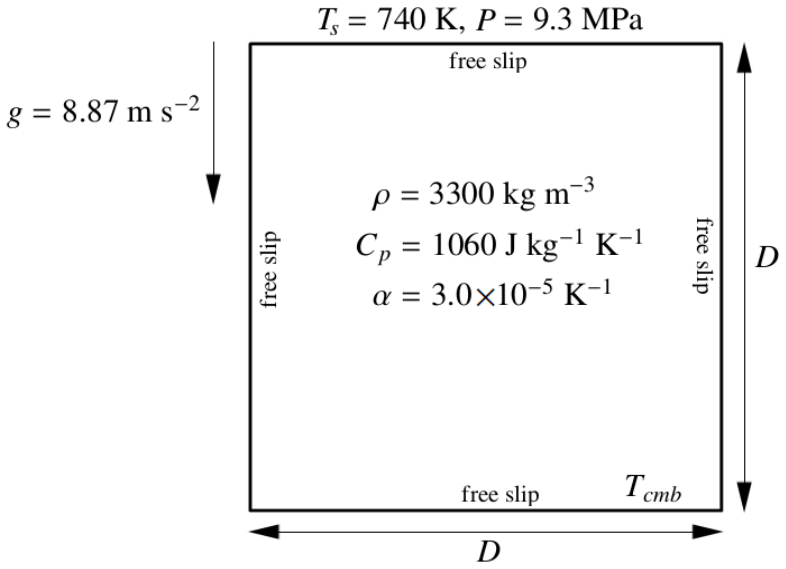

Figure 6: Model setup: boundary conditions and constant material properties are indicated. The thickness of the mantle D is varied in the modelling study, as is the core-mantle boundary temperature T_{cmb}.

conditions of the side-walls insulation is assumed, i.e. $\partial T/\partial x = 0$.

To initiate the model, an initial temperature distribution of the temperature field is prescribed:

$$T(x,y) = T_s + (D-y)\cdot\frac{T_{cmb}-T_s}{D} + \frac{T_{cmb}}{100}\cdot\cos\left(\frac{\pi x}{D}\right)\cdot\sin\left(\frac{\pi\cdot(D-y)}{D}\right). \quad (14)$$

Here, $T_{cmb}/100$ is the amplitude of the initial perturbation in the temperature distribution.

Following Tosi et al. (2015), the viscosity is calculated using harmonic averaging between a linear viscosity μ_{lin} that only depends on temperature and depth and a plastic, non-linear viscosity μ_{plast} that depends on the strain rate:

$$\mu(T,y,\dot{\boldsymbol{\varepsilon}}) = 2\left(\frac{1}{\mu_{lin}(T,y)} + \frac{1}{\mu_{plast}(\dot{\boldsymbol{\varepsilon}})}\right)^{-1}. \quad (15)$$

In this equation, the linear viscosity is given by the following formula (Tosi et al., 2015):

$$\mu_{lin}(T,y) = \exp\left(-\gamma_T\cdot\frac{T-T_s}{T_{cmb}-T_s}T + \gamma_y\cdot\frac{y}{D}\right), \quad (16)$$

where $\gamma_T = \ln(\Delta\mu_T)$ and $\gamma_y = \ln(\Delta\mu_y)$. These parameters control the total viscosity contrast in the system due to temperature ($\Delta\mu_T$) and pressure ($\Delta\mu_y$). Following Tosi et al. (2015), the viscosity contrast due to temperature was chosen to be $\Delta\mu_T = 10^5$ Pa s and the depth-dependent velocity contrast was chosen to be $\Delta\mu_y = 10$ Pa s.

The non-linear, plastic viscosity is given by

$$\mu_{plast}(\dot{\boldsymbol{\varepsilon}}) = \mu^* + \frac{\sigma_Y}{\sqrt{\dot{\boldsymbol{\varepsilon}}:\dot{\boldsymbol{\varepsilon}}}} \quad (17)$$

with

$$\sqrt{\dot{\boldsymbol{\varepsilon}}:\dot{\boldsymbol{\varepsilon}}} = \sqrt{\dot{\varepsilon}_{ij}\dot{\varepsilon}_{ij}} = \sqrt{\left(\frac{\partial u_x}{\partial x}\right)^2 + \frac{1}{2}\left(\frac{\partial u_x}{\partial y} + \frac{\partial u_y}{\partial x}\right)^2 + \left(\frac{\partial u_y}{\partial y}\right)^2}. \quad (18)$$

In this equation μ^* represents the effective viscosity at high stresses and σ_Y is the yield stress. Both quantities are assumed to be constant, after Tosi et al. (2015). The value for μ^* is 10^{24}, which results from dimensionalizing the Tosi et al. (2015) quantity. Yield stresses are varied to investigate which mantle convective regime is dominant for a certain yield stress. It is expected that a low yield stress results in an easily breakable upper lid which results in a mobile lid regime. High yield stresses would probably result in the stagnant lid regime with a rigid upper lid. The periodic regime is expected for intermediate yield stresses (Tosi et al., 2015).

In order to investigate the influence of temperature- and pressure-dependent conductivity, models are run with either a constant conductivity of k = 3.5 W m^{-1} K^{-1} or a variable conductivity, following Hofmeister (1999) and van den Berg et al. (2001):

$$k(T,P) = k_0\left(\frac{740}{T}\right)^a\exp\left[-\left(4\gamma+\frac{1}{3}\right)\alpha(T-740)\right]\left(1+\frac{K_0'P}{K_0}\right) + 0.0175 - 0.0001037T + \frac{2.245T^2}{10^7} - \frac{3.407T^3}{10^{11}} \quad (19)$$

Because there are no constraints on the various constants in this equation for Venus, it is assumed that Venus and Earth are similar with regards to these parameters. So, in equation (19)

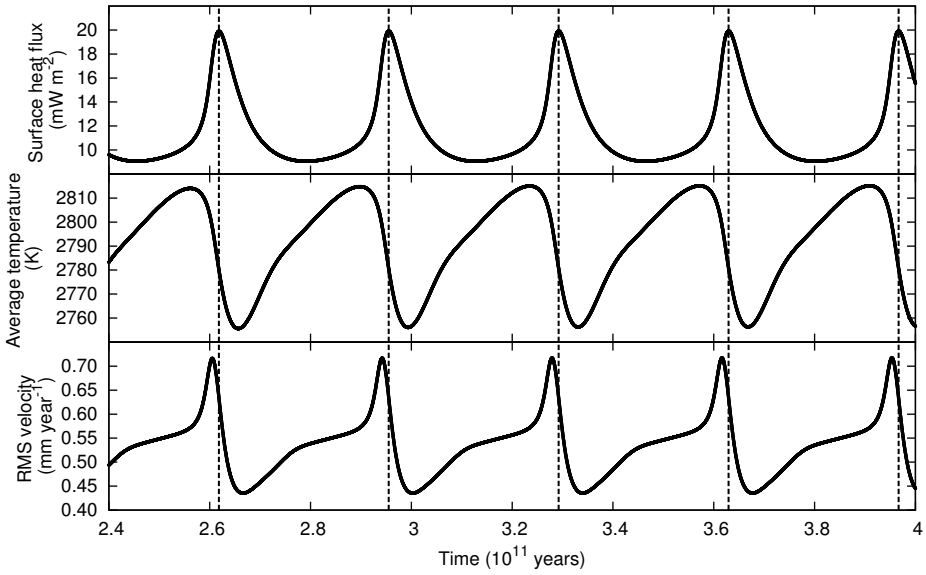

Figure 7: Time series of the surface heat flux, average temperature and RMS velocity after the system reached a strictly periodic regime. These results are for a model with mantle thickness D = 3100 km, core-mantle boundary temperature T_{cmb} = 3850 K and yield stress σ_Y = 375 MPa.

the constants that are used are $k_0 = 4.7$ W m^{-1} K^{-1}, $a = 0.3$, $\gamma = 1.2$, $\alpha = 2.0 \times 10^{-5}$ K^{-1}, $K_0 = 261 \times 10^9$ Pa and $K_0' = 5$ (also see Table 5 for an explanation of the parameters).

In this study, the thickness of the mantle D was varied from D = 2600 km to D = 3600 km (after Yoder (1995)) and the core-mantle boundary temperature T_{cmb} was varied from T_{cmb} = 3200 K to T_{cmb} = 4500 K (Schubert et al., 2001). The resolution that was used for all the models is 64×64. No higher resolution was needed, because it was shown in Tosi et al. (2015) that the resolution of a model in ASPECT does not influence the results.

8. Results

In this section the results of the modelling study are presented. First, the three mantle convective regimes that are obtained with these models are discussed, after which the influence of the thickness of the mantle D, the core-mantle boundary temperature and the temperature-dependent conductivity are discussed. Lastly, the results for the subcrustal lid rejuvenation model of Ghail (2015) are presented.

8.1. The three mantle convective regimes

For each model with different D and T_{cmb} (see Section 8.2 and 8.3) the yield stress σ_Y was varied in order to determine the critical yield stresses at which the system changes its mantle convective regime. It was found that for low values of σ_Y the system typically develops into a mobile lid regime (see Figure 9) in which the top part of the mantle, which behaves plastically, moves along the surface. For high yield stresses, the system develops into a stagnant lid regime, where heat transport is mainly accommodated through conduction. For intermediate yield stresses, a periodic regime develops (see Figure 7). Note that the maxima of the average temperature in Figure 7 are out of phase with the the maxima of the surface heat flux and RMS velocity. The reason for this is that during the drop in temperature, the mantle is overturning which results in a high RMS velocity and surface heat flux. An example which illustrates the transition of mantle convective regimes with yield stress is given in Figure 8 for a model with D = 3600 km and T_{cmb} = 4500 K.

8.2. Mantle thickness

Models have been run with a mantle thickness D of 3600 km, 3100 km and 2600 km in order to investigate the influence of the mantle thickness on the transitions of mantle convection regimes (see Figure 10). It appears as if the transition from mobile lid regime to periodic regime occurs at a lower yield stress, when the thickness of the mantle is increased. Furthermore, the transition from periodic regime to stagnant lid regime occurs at a higher yield stress for increasing D. Indeed, when the mantle is too thin, there is no periodic regime at all, but instead there is a transition zone between the mobile lid regime and the stagnant lid regime. In this transition zone, the upper thermal boundary layer moves very slowly, thereby resembling both the mobile lid regime in part and the stagnant lid regime (see Figure 9). From these models, it appears as if the thickness of the mantle D is a controlling factor regarding the range of yield stresses that result in a periodic regime. Besides that, Figure 10 shows that an increase in mantle thickness also reduces the period of overturn.

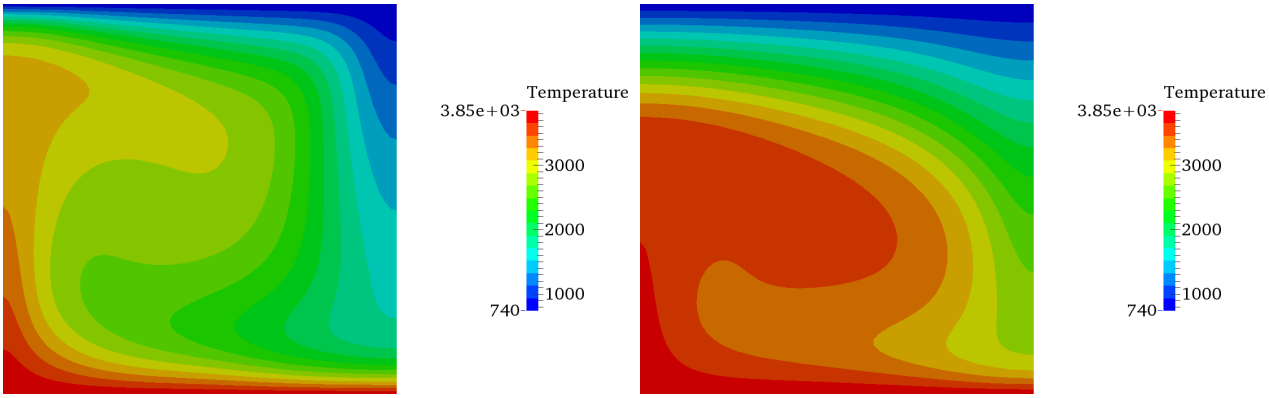

(a) Temperature field of the mobile lid regime

(b) Temperature field of the stagnant lid regime

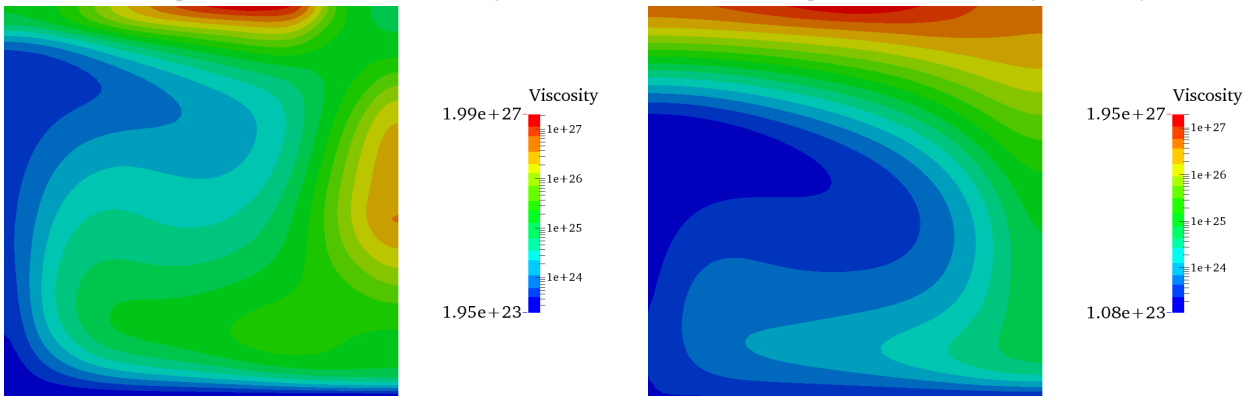

(c) Viscosity field of the mobile lid regime

(d) Viscosity field of the stagnant lid regime

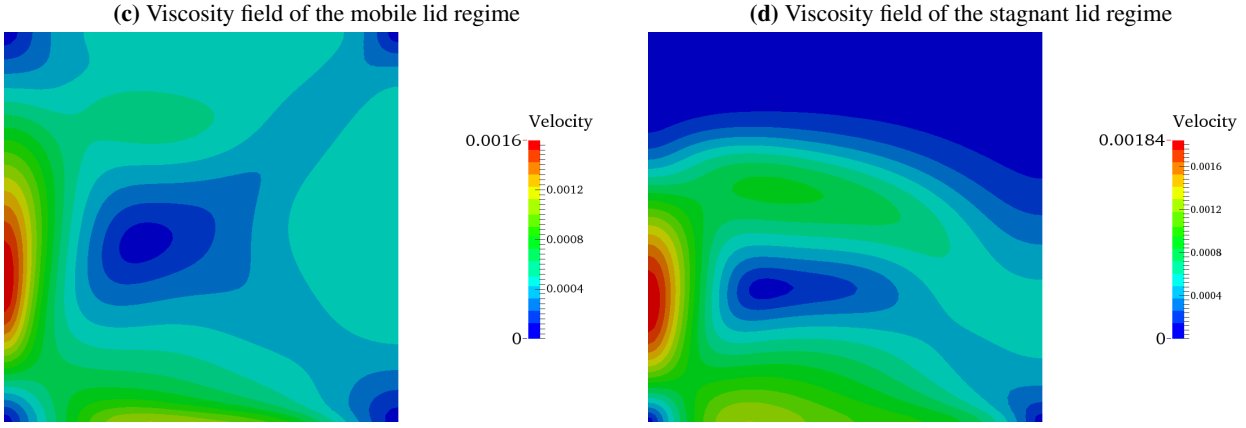

(e) Velocity field (magnitude) of the mobile lid regime

(f) Velocity field (magnitude) of the stagnant lid regime

Figure 9: Representative mobile lid (left) and stagnant lid (right) models when they have reached steady state. Both models have a mantle thickness D = 3100 km and a core-mantle boundary temperature T_{cmb} = 3850 K. Yield stress for the mobile lid model is σ_Y = 200 MPa, while the yield stress for the stagnant lid model is σ_Y = 500 MPa.

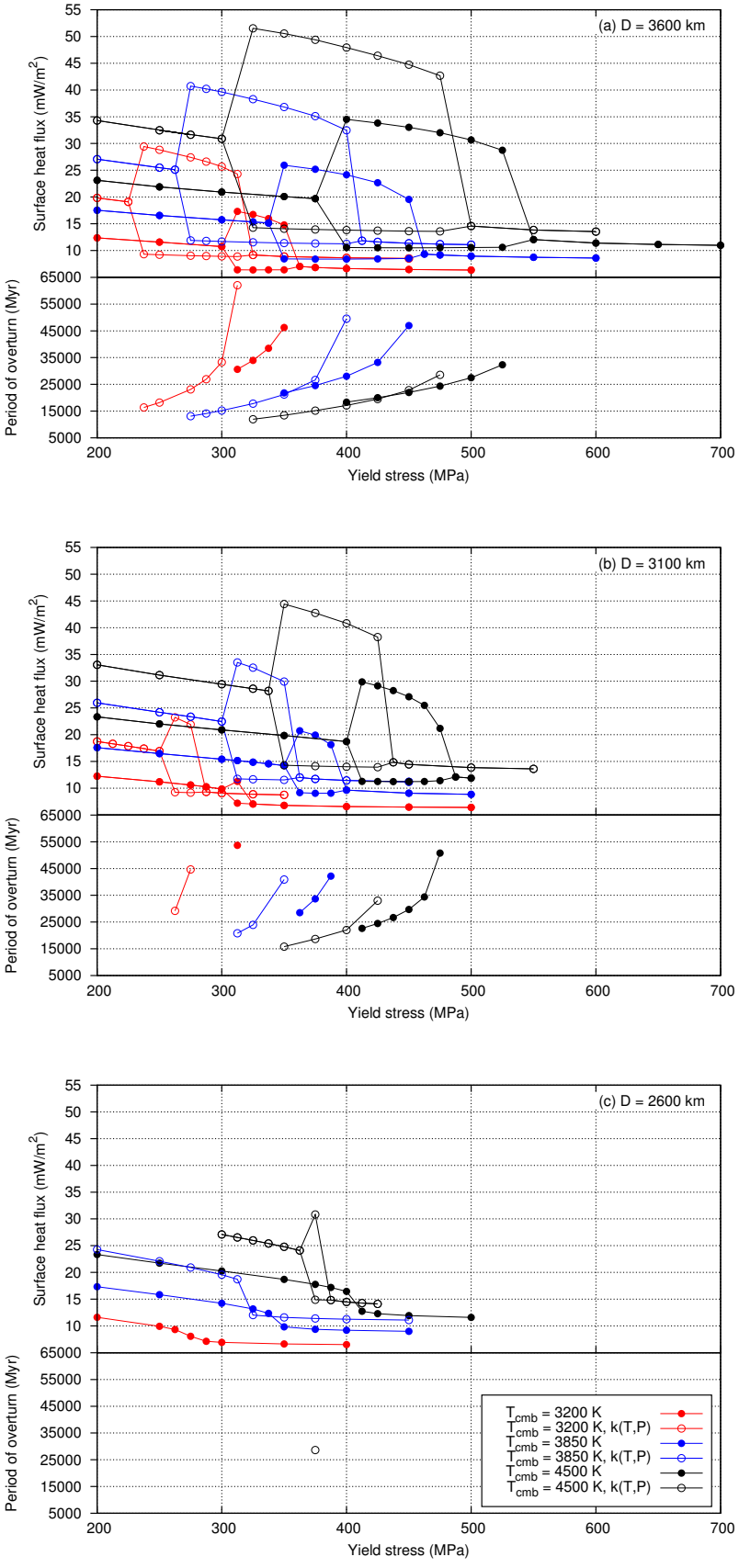

Figure 10: Results of all standard (i.e., not subcrustal lid) models. (a) Models with D = 3600 km for different values of T_{cmb} with (solid dots) and without (open dots) temperature-dependent conductivity. (b) Similar to (a) but with D = 3100 km. (c) Similar to (a) but with D = 2600 km.

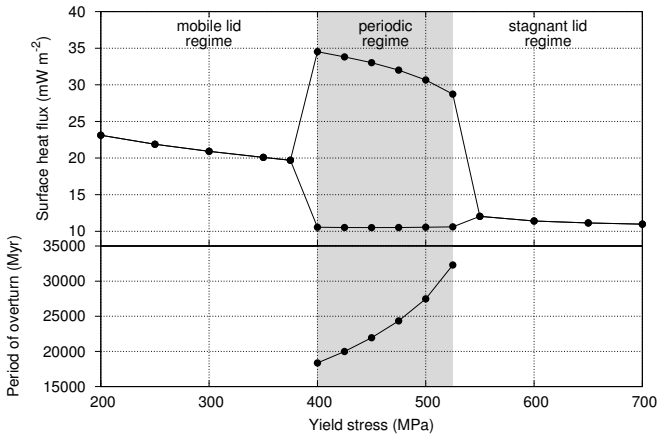

Figure 8: The surface heat flux as a function of yield stress for a model with mantle thickness D = 3600 km and core-mantle boundary temperature T_{cmb} = 4500 K. Different yield stresses result in different mantle convective regimes (indicated): a mobile lid regime (see Figure 9), a periodic regime (grey, see Figure 7) or a stagnant lid regime (see Figure 9). The surface heat fluxes in the periodic regime are the maximum and minimum surface heat flux in a cycle (see also Figure 7). The period of overturn is indicated for the models with a periodic regime.

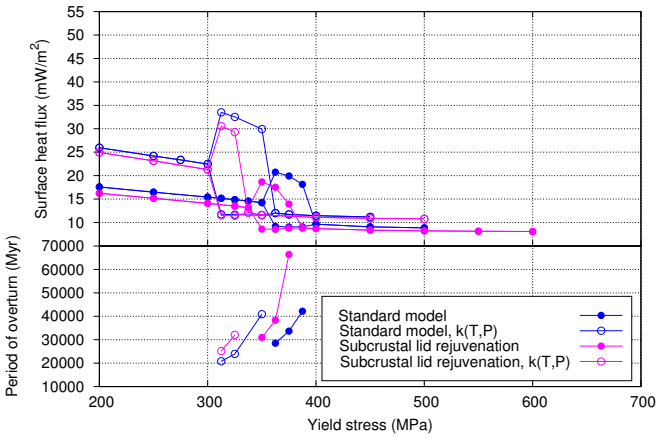

Figure 11: Results of the subcrustal lid models for a mantle thickness D = 3100 km and a core-mantle boundary temperature of T_{cmb} = 3850 K compared to the standard models for the same mantle thickness and core-mantle boundary temperature.

8.3. Core-mantle boundary temperature

The different core-mantle temperatures T_{cmb} that were used to investigate the influence on the mantle convective regimes are T_{cmb} = 3200 K, T_{cmb} = 3850 K and T_{cmb} = 4500 K. As was to be expected, a higher core-mantle boundary temperature results in an overall higher surface heat flux as can be seen in Figure 10. Besides that, similar to the results of the mantle thickness, an increase in core-mantle boundary temperature results in a larger range of yield stresses in which the periodic regime is stable. Also note that the critical yield stress which marks the transition between the mobile lid regime and the periodic regime shifts to larger yield stresses for increasing core-mantle boundary temperature. Similarly, the transition zone between the mobile lid and the stagnant lid regime for models with a thin mantle shifts towards larger yield stresses.

The period of overturn seems not to be affected much by the change in core-mantle boundary temperature, although the range of the periods of overturn increases with increasing. However, this is also partly due to the increase in the range of yield stresses for which a periodic regime is stable.

8.4. Temperature-dependent thermal conductivity

Using a temperature- and pressure-dependent thermal conductivity k instead of a constant conductivity results in an increase in overall surface heat flux (see Figure 10). Besides that, the critical yield stress at which the transition from mobile lid regime to periodic regime occurs shifts to lower yield stresses. In line with that, the range of yield stresses at which the periodic regime is dominant increases when a temperature-dependent conductivity is used. The period of overturn decreases slightly when a temperature-dependent conductivity is used. In Figure 10 there is no model that includes a temperature-dependent conductivity for D = 2600 km and T = 3200 K, because the model lacked a driving force and therefore, did not develop. Therefore, this model with such a thin mantle and low core-mantle boundary temperature is considered unlikely for Venus.

8.5. Subcrustal lid rejuvenation models

The results for the subcrustal lid rejuvenation models are shown in Figure 11. The subcrustal lid models were only run for the typical, average mantle thickness D = 3100 km and core-mantle boundary T_{cmb} = 3850 K. Remarkably, the results from the subcrustal lid models show a trend that is in contrast with the standard models, concerning the incorporation of the temperature dependent conductivity. Where the standard models usually show an increase in the range of yield stresses for which the periodic regime is stable when the temperature dependent conductivity is incorporated, the subcrustal lid regime shows a decrease. Other than that, the values of the heat fluxes are fairly similar. Hence, this modelling study indicates that the subcrustal lid regime is indeed physically possible and could account for the heat loss of Venus.

9. Discussion

The results show that the mantle thickness, the core-mantle boundary temperature and the temperature dependent conductivity mainly affect the range of yield stresses for which a periodic regime is stable and the critical yield stresses which mark the transition from the mobile lid regime to the periodic regime and the transition from the periodic regime to the stagnant lid regime. In this section, the modelling study that was conducted is surveyed critically and compared to previous studies. Furthermore, exploratory models are presented that aim towards complexifying the current model and possible future research directions are suggested in line with that.

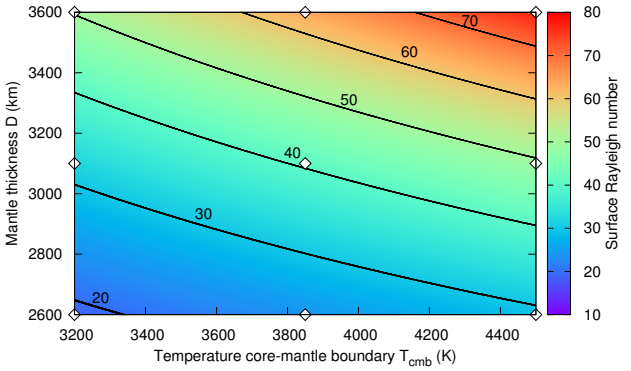

Figure 12: Surface Rayleigh numbers for different mantle thicknesses D and core-mantle boundary temperatures T_{cmb}. Contour lines of Rayleigh numbers are indicated. The nine models tested in this study are indicated by white diamonds.

9.1. Rayleigh number

In order to explain the increase in the range of the yield stresses under which the periodic regime is stable for increasing mantle thickness and core-mantle boundary temperature, the Rayleigh number can be used. The Rayleigh number is defined as (Tosi et al., 2015):

$$Ra = \frac{\rho g \alpha \Delta T D^3}{\mu \kappa} \tag{20}$$

where ρ is the density, g is the gravity acceleration, α is the thermal expansion coefficient, ΔT is the temperature difference in the system $T_{cmb} - T_s$, D is the mantle thickness, μ is the viscosity and κ is the thermal diffusivity defined as:

$$\kappa = \frac{k}{\rho C_p} \tag{21}$$

where k is the thermal conductivity and C_p is the heat capacity. Calculations of the surface Rayleigh number for a range of possible mantle thicknesses and core-mantle boundary temperatures with $\rho = 3300$ kg m^{-3}, $g = 8.87$ m s^{-2}, $\alpha = 3.0 \times 10^{-5}$ K^{-1}, $T_s = 740$ K, μ at the surface is 2×10^{27} Pa s, $k = 3.5$ W m^{-1} K^{-1} and $C_p = 1060$ J kg^{-1} K^{-1} are shown in Figure 12. The viscosity contrast due to temperature of $\Delta\mu_T = 10^5$ Pa s ultimately results in a maximum Rayleigh number of $\sim 7.7 \times 10^6$ at the bottom of the mantle.

The increase of the range of yield stresses in which the periodic regime is stable can be explained by an increase in Rayleigh number which results from an increase in core-mantle boundary temperature or mantle thickness. The reason for this is that a mantle with a higher Rayleigh number convects more rigorously, which in turn makes it easier to overturn the whole mantle, even though the yield stress is quite high. Because the definition of the Rayleigh number contains D^3 it is evident why the mantle thickness is more important for the critical yield stress than the core-mantle boundary temperature.

Even so, the Rayleigh number cannot solely explain the results in Figure 10 as the ratio between the thickness of the mantle and the temperature at the core-mantle boundary seems to be important as well. An example of this is provided by two models with approximately the same surface Rayleigh number of 50. A comparison between these two models (a model with $D = 3600$ km and $T_{cmb} = 3200$ K and a model with $D = 3100$ and $T_{cmb} = 4500$ K) shows that a higher T_{cmb}, regardless of the Rayleigh number, still causes an increase in surface heat flux and an increase in the range of yield stresses for which the periodic regime is stable. Furthermore, the model with a thick mantle has a smaller critical yield stress for the transition between the mobile lid and periodic regime than the model with a thinner mantle.

Hence, even though the Rayleigh number plays a role, the mantle thickness D and core-mantle boundary temperature T_{cmb} ultimately determine the value of the critical yield stresses.

9.2. Subcrustal lid rejuvenation models

The results for the subcrustal lid rejuvenation models are not significantly different from the standard models, although this would be expected considering the significant change in boundary conditions at the top, i.e. $T_s = 900$ K instead of $T_s = 740$ K and $P = 300$ MPa instead of $P = 9.3$ MPa. The reason for the minimum amount of change between these two models is that the rheology that is used in these models is not pressure dependent. So, even though the largest difference between the models is the pressure, the model does not change. For a temperature- and pressure-dependent conductivity, the subcrustal lid rejuvenation model indeed shows a more significant change. It is expected that future models with a more complex rheology that is also pressure dependent would capture the process of subcrustal lid rejuvenation better.

9.3. Evolution of the models

The results shown in Section 8 typically display the mantle convection regime after the model has reached steady state. However, it is unknown whether Venus has already reached steady state at present or not. Therefore, it might be useful to look at the entire time evolution of the mantle models. Three typical time evolutions in Figure 13 show the various ways in which models develop before they reach steady state. It is particularly interesting that some models show one or a few mantle overturns before reaching a steady state stagnant lid regime (see Figure 13(a) for an example). This evolution would be in line with the hypothesis of surface quiescence after the last global resurfacing event (see Section 5.2.1). Other models that reach a 'steady state' with a constant period (see Figure 13(c)) of overturn back the hypothesis of global episodic subduction (see Section 5.2.2). Not shown in Figure 13 are the models that reach a steady state stagnant lid or mobile lid regime without global mantle overturns in their early history. These models verify the uniformitarian model.

From these different model results, it is clear that the variously proposed thermal evolution models of Venus can be modelled physically. The key factors that determine the mantle evolution are ultimately the mantle thickness D, the core-mantle

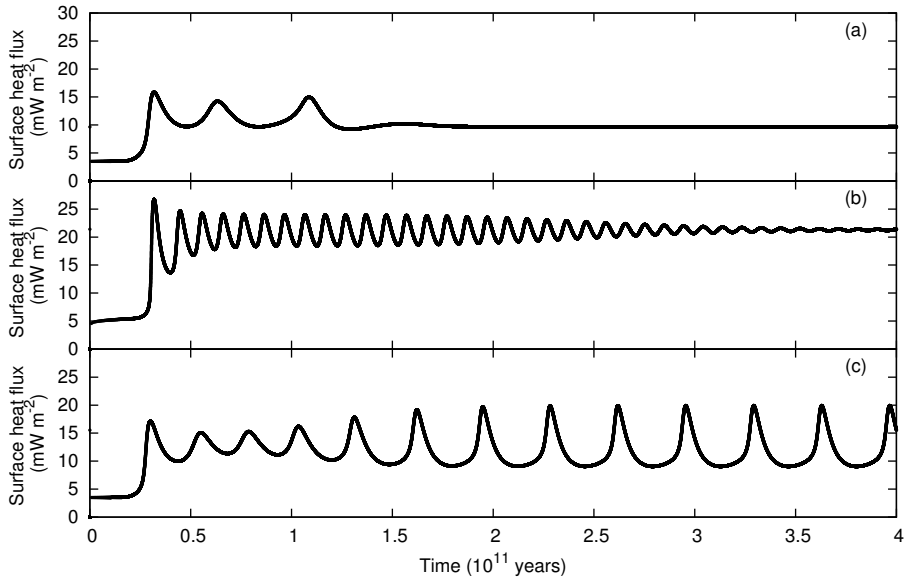

Figure 13: The entire time evolution of three resentative models: (a) Standard model for D = 3100 km, T_{cmb} = 3850 K, and σ_Y = 400 MPa. After three initial mantle overturns, the model reaches the steady state stagnant lid regime; (b) Subcrustal lid rejuvenation model for D = 3100 km, T_{cmb} = 3850 K, and σ_Y = 300 MPa. Initially, the model is periodic with a period of mantle overturn of ∼ 10000 Myr, but the model converges to the steady state stagnant lid regime; (c) Standard model for D = 3100 km, T_{cmb} = 3850 K, and σ_Y = 375 MPa. The model develops a fully stable periodic regime, although the periodicity only becomes constant after approximately 1.5×10^{11} years.

boundary T_{cmb} and the yield stress σ_Y of the lithosphere. When future space missions to Venus acquire more information on these parameters, the parameter study conducted in this work could help determine what thermal evolution Venus experienced.

9.4. Period of overturn

The models predict a period of mantle overturn of 15000 up to 55000 Myr. This is similar to the scaled periods of overturn of 10660 Myr (Trompert and Hansen, 1998) and ∼ 20480 Myr (Tosi et al., 2015). However, these values for the period of overturn are not realistic, as the studies concerning the age of the surface of Venus (see Section 3.2) generally predict that the time since the last overturn is 300 to 800 Myr. Besides that, the age of Venus is approximately 4600 Myr (like Earth), so a periodic regime in which the period of overturn exceeds 4600 Myr is unrealistic or simply implies that Venus hasn't experienced a mantle overturn yet. The latter is however very unlikely, because of the impact crater evidence (see Section 3.2). Therefore, the likely explanation for the large period of overturn predicted by these models is a deficiency of the models. There are several possible reasons why the model cannot capture a realistic period of overturn. It could be that there is not enough heat supply for a fast mantle convection and period of overturn, because of the omission of internal heat production, frictional heating and adiabatic heating. Furthermore, the time stepping may be too large to capture a short period of overturn. Future modelling studies should focus on the effect of the incorporation of internal, frictional and adiabatic heating in order to see whether a smaller and more realistic period of overturn can be obtained (see also Section 9.6).

9.5. Surface heat flux

The surface heat flux that is predicted by the models presented in Section 8 are lower than the expected present-day surface heat flux of approximately 74 mW m^{-2} (see Section 5). The simplicity of the models may be the cause for this, as several additional sources of heat, such as the shear heating, adiabatic heating and internal heat production, are omitted from these models. Therefore, it is expected that future models that incorporate these features provide surface heat fluxes that are more comparable to the estimated present-day surface heat flux (see also Section 9.6).

However, the minimum surface heat flux that is predicted by the models for a mantle thickness D = 3100 km and D = 3600 km for the periodic regime, matches with the theoretically predicted surface heat fluxes of 11.1 mW m^{-2} (see Section 5). This result tends to lend some support to the notion that the models presented in this work capture the most essential processes of Venus mantle convection in the periodic regime.

9.6. Shear heating

In order to test the influence of extra sources of heat as discussed in Section 9.4 and 9.5, a set of preliminary models was run which incorporates shear heating for a mantle thickness D = 3100 km and a core-mantle boundary temperature T_{cmb} = 3850 K. The results of these models are shown in Figure 15. Clearly, the incorporation of shear heating effects the model

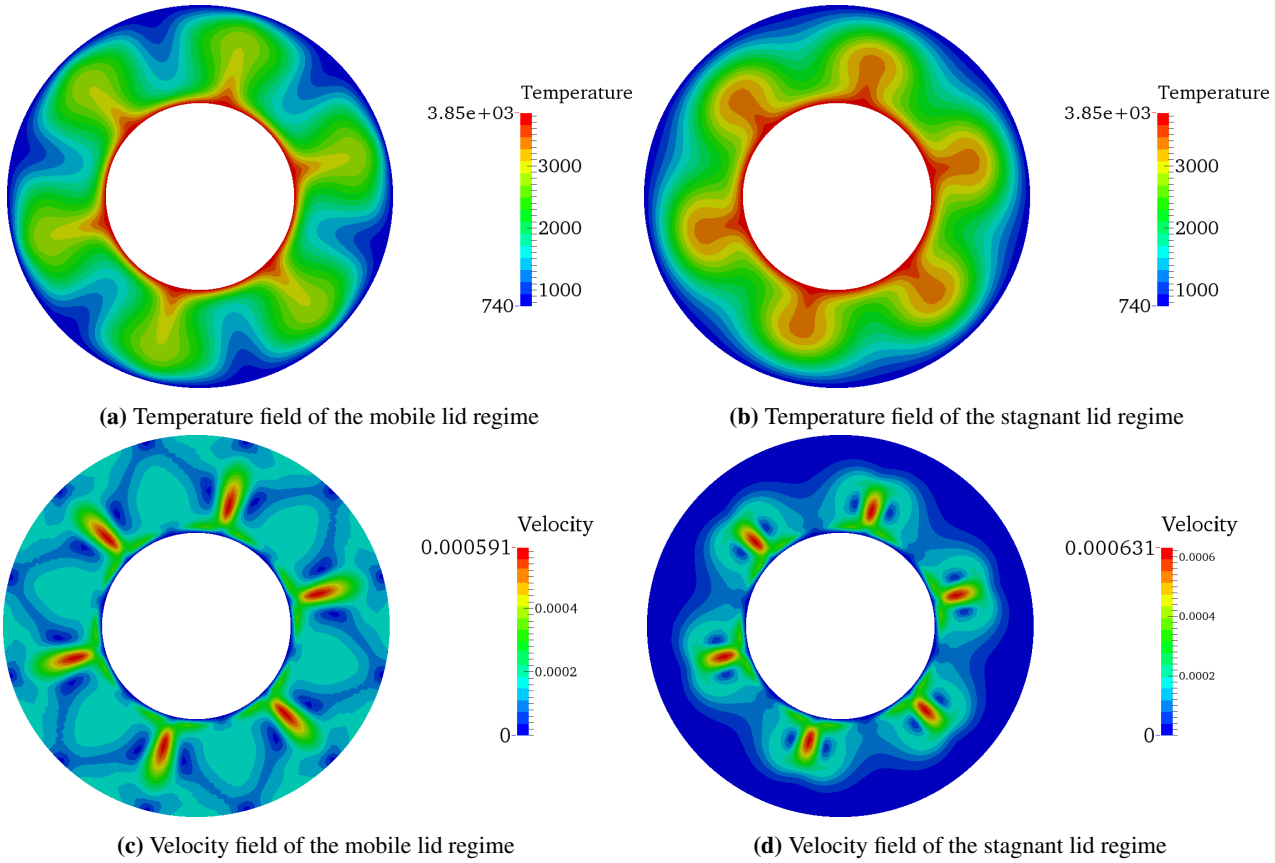

(a) Temperature field of the mobile lid regime

(b) Temperature field of the stagnant lid regime

(c) Velocity field of the mobile lid regime

(d) Velocity field of the stagnant lid regime

Figure 14: Representative results for a cylindrical model. The mobile lid regime model (left) was run with a yield stress $\sigma_Y = 200$ MPa and the stagnant lid model (right) with a yield stress $\sigma_Y = 550$ MPa.

significantly. Most importantly, the periodic regime occurs at much lower yield stresses σ_Y for models including shear heating than models without shear heating. Besides that, the period of overturn is lower as well. These findings support the hypothesis that more advanced models that incorporate shear heating, adiabatic heating and internal heat production could capture the processes in the mantle of Venus better. More specifically, a realistic value for the period of overturn could possibly be obtained by the use of more complex models. Besides that, the incorporation of shear heating results in a higher predicted surface heat flux. This supports the assumption that future models which incorporate additional heat sources will provide heat fluxes that are better comparable to the estimated present-day heat flux (see Section 9.5).

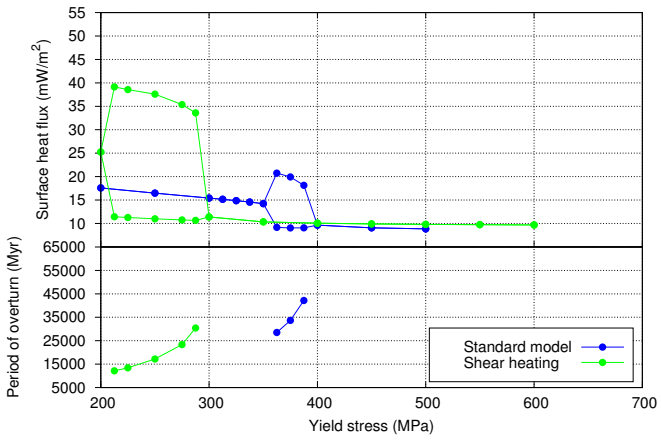

Figure 15: Preliminary results for models that incorporate shear heating.

9.7. Cylindrical models

Although the two dimensional Cartesian models used in this work are very well suited for parameter studies concerning the mantle of Venus, more realistic models are ideally spherical and three dimensional. In order to investigate how the findings of the two dimensional Cartesian models would translate to a two dimensional cylindrical model a set of preliminary cylindrical models was run with a mantle thickness $D = 3100$ km and a core-mantle boundary temperature $T_{cmb} = 3850$ K. The resolution is lower than the Cartesian models, due to a time constraint. The initial temperature distribution is a hexagonal perturbation, analogous to the sine perturbation in the Cartesian models. The results are presented in Figure 16 and representative models of the mobile lid and stagnant lid regime are shown in Figure 14.

Unlike the Cartesian models, the cylindrical models do not retrieve the periodic regime for the mantle thickness $D = 3100$ km and core-mantle boundary temperature $T_{cmb} = 3850$ K. Instead, they are more comparable to the Cartesian models with

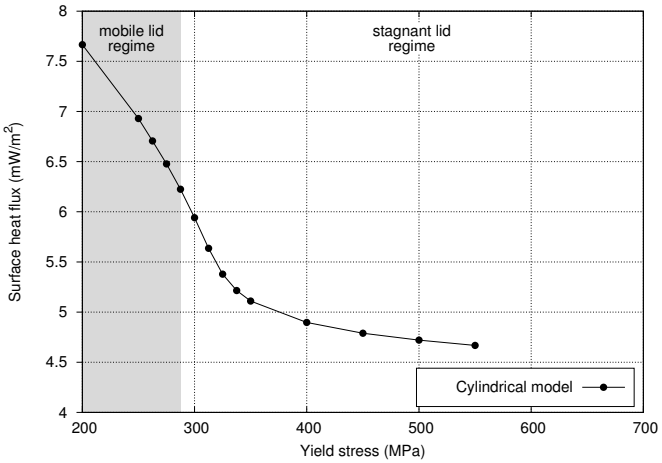

Figure 16: Preliminary results for cylindrical models.

mantle thickness $D = 2600$ km. The reason for this is probably that there is not enough heat in the cylindrical model to act as a driving force for the periodic regime. The lack of heating results from the fact that the area of the studied domain is much larger in the cylindrical model ($\sim 87,689,390$ km) than in the Cartesian model ($9,610,000$ km), even though the mantle thickness D is the same. It is expected that future models that incorporate internal heat production, frictional heating and adiabatic heating will result in the ability of the cylindrical models to capture the periodic regime as well.

10. Conclusion

Venus is an important planet to study as the evolution of this planet could shed some light on why Earth is such a unique planet. However, it is difficult to obtain observations and data from Venus, as the planet is covered in clouds. Therefore, the most efficient method of acquiring data is the use of space missions. In the past, space missions such as Pioneer Venus and Magellan have mapped approximately 98% of the surface of Venus, which resulted in information about the impact crater distribution. As this distribution is indistinguishable from a random distribution, a global resurfacing event $\sim$ 500 Myr ago has been hypothesized to account for this. Several thermal evolution hypotheses, such as the uniformitarian, catastrophic, differentiated planet and subcrustal lid rejuvenation hypothesis have been proposed in order to explain Venus' thermal evolution together with the global resurfacing event. In order to validate these hypotheses, modelling studies have been conducted. However, several important parameter studies were neglected in these modelling studies. For example, few modelling studies have investigated the influence of the mantle thickness or core-mantle boundary on the mantle convective regime of Venus, while these parameters are largely unconstrained. Furthermore, no studies have been conducted with a temperature-dependent conductivity. Therefore, a modelling study was conducted to study the aforementioned parameters.

It was found that the models retrieve the three mantle convective regimes: mobile lid, periodic, and stagnant lid. The period of overturn is unrealistic, but future models that incorporate shear heating, adiabatic heating and internal heat production, should be able to capture more realistic periods of overturn. The mantle thickness influences whether a periodic regime can be obtained for a range of yield stresses. More specifically, a thin mantle ($\sim$ 2600 km) cannot accommodate a periodic regime, while thicker mantles can. To a lesser extent, the core-mantle boundary temperature influences this as well. Hence, it is important to investigate the effect of mantle thickness and core-mantle boundary temperature on the model results, in order to prevent biased results.

The temperature-dependent conductivity results in the occurrence of the periodic regime at lower yield stresses and over a larger range of yield stresses. Therefore, future modelling studies should incorporate the temperature-dependent conductivity to ensure that the periodic regime occurs at the correct yield stress.

The subcrustal lid rejuvenation models showed for the first time that the hypothesis proposed by Ghail (2015) can be numerically validated. The difference between the standard model and subcrustal lid rejuvenation model is small, because of a rheology that is not pressure dependent.

All in all, this study has shown that in order to understand more about Venus' mantle dynamics, it is important to study the effects of the most basic parameters, such as mantle thickness and core-mantle boundary temperature, because they can significantly influence the results. Besides that, the incorporation of a temperature-dependent conductivity could be yet another addition to models in order to make them more realistic.

Future models should focus on the incorporation of additional heat sources in the model, such as shear heating, adiabatic heating and internal heat production. Furthermore, the addition of a pressure dependent rheology could significantly improve the subcrustal lid rejuvenation models.

Acknowledgements

While writing this work, I received the help of many people. I'd like to thank my daily supervisor Cedric Thieulot, who helped with the modelling and provided feedback on my initial version. I am also thankful to Richard Ghail, who proved to be a valuable source of knowledge concerning Venus and helped to greatly improve my literature study. I'd also like to thank my official first supervisor Arie van den Berg who, indeed, did a 'duit in het zakje'. Anne Glerum helped during the start of this project with setting up the model correctly, for which I am very grateful. Then last but not least, my loyal roommates Maurits Metman and Jasper Ploegstra at the university deserve thanks for the fruitful (and not-so-fruitful) discussions and the feedback I received from them on numerous preliminary and not-so-preliminary versions of my thesis. Thank you!

References

Ainsworth, J. and Herman, J. (1975). Venus wind and temperature structure: The venera 8 data. *Journal of Geophysical Research*, 80(1):173–179.

Aitta, A. (2012). Venus internal structure, temperature and core composition. *Icarus*, 218(2):967–974.

Anderson, F. S. and Smrekar, S. E. (2006). Global mapping of crustal and lithospheric thickness on venus. *Journal of Geophysical Research: Planets (1991–2012)*, 111(E8).

Arkani-Hamed, J. (1994). On the thermal evolution of venus. *Journal of Geophysical Research: Planets*, 99(E1):2019–2033.

Arkani-Hamed, J. and Toksöz, M. (1984). Thermal evolution of Venus. *Physics of the earth and planetary interiors*, 34(4):232–250.

Armann, M. and Tackley, P. J. (2012). Simulating the thermochemical magmatic and tectonic evolution of venus's mantle and lithosphere: Two-dimensional models. *Journal of Geophysical Research: Planets (1991–2012)*, 117(E12).

Avduevsky, V., Marov, M. Y., and Rozhdestvensky, M. (1970). A tentative model of the venus atmosphere based on the measurements of veneras 5 and 6. *Journal of the Atmospheric Sciences*, 27(4):561–568.

Avduevsky, V., Marov, M. Y., Rozhdestvensky, M., Borodin, N., and Kerzhanovich, V. (1971). Soft landing of venera 7 on the venus surface and preliminary results of investigations of the venus atmosphere. *Journal of the Atmospheric Sciences*, 28(2):263–269.

Bangerth, W., Heister, T., et al. (2015). ASPECT*: Advanced Solver for Problems in Earth's ConvecTion*. Computational Infrastructure for Geodynamics.

Basilevsky, A. (1993). Age of rifting and associated volcanism in atla regio, venus. *Geophysical research letters*, 20(10):883–886.

Basilevsky, A. T. and Head, J. W. (1998). The geologic history of venus: A stratigraphic view. *Journal of Geophysical Research: Planets (1991–2012)*, 103(E4):8531–8544.

Bilotti, F. and Suppe, J. (1999). The global distribution of wrinkle ridges on venus. *Icarus*, 139(1):137–157.

Bougher, S. W., Hunten, D. M., and Phillips, R. J. (1997). *Venus II–geology, Geophysics, Atmosphere, and Solar Wind Environment*, volume 1. University of Arizona Press.

Bullock, M. A., Grinspoon, D. H., and Head, J. W. (1993). Venus resurfacing rates: Constraints provided by 3-d monte carlo simulations. *Geophysical research letters*, 20(19):2147–2150.

Dickey, J. et al. (1997). Satellite gravity and the geosphere: Contributions to the study of the solid earth and its fluid envelope, 112 pp. *Natl. Acad. Press, Washington, DC*.

Dorn, C., Khan, A., Heng, K., Alibert, Y., Benz, W., Connolly, J. A., and Tackley, P. (2014). Can we constrain interior structure of rocky exoplanets from mass and radius measurements?

Drossart, P., Piccioni, G., Adriani, A., Angrilli, F., Arnold, G., Baines, K., Bellucci, G., Benkhoff, J., Bézard, B., Bibring, J.-P., et al. (2007). Scientific goals for the observation of venus by virtis on esa/venus express mission. *Planetary and Space Science*, 55(12):1653–1672.

Esposito, L. W., Copley, M., Eckert, R., Gates, L., Stewart, A., and Worden, H. (1988). Sulfur dioxide at the venus cloud tops, 1978–1986. *Journal of Geophysical Research: Atmospheres (1984–2012)*, 93(D5):5267–5276.

Florensky, C., Basilevsky, A., Kryuchkov, V., Kusmin, R., Nikolaeva, O., Pronin, A., Chernaya, I., Tyuflin, Y. S., Selivanov, A., Naraeva, M., et al. (1983). Venera 13 and venera 14: sedimentary rocks on venus? *Science*, 221(4605):57–59.

Florensky, C., Ronca, L., Basilevsky, A., Burba, G., Nikolaeva, O., Pronin, A., Trakhtman, A., Volkov, V., and Zazetsky, V. (1977). The surface of venus as revealed by soviet venera 9 and 10. *Geological Society of America Bulletin*, 88(11):1537–1545.

Ford, P. G. and Pettengill, G. H. (1992). Venus topography and kilometer-scale slopes. *Journal of Geophysical Research: Planets (1991–2012)*, 97(E8):13103–13114.

Gerya, T. (2014). Plume-induced crustal convection: 3d thermomechanical model and implications for the origin of novae and coronae on venus. *Earth and Planetary Science Letters*, 391:183–192.

Ghail, R. (2015). Rheological and petrological implications for a stagnant lid regime on venus. *Planetary and Space Science*.

Gillmann, C. and Tackley, P. (2014). Atmosphere/mantle coupling and feedbacks on venus. *Journal of Geophysical Research: Planets*, 119(6):1189–1217.

Glassmeier, K.-H., Soffel, H., and Negendank, J. (2008). *Geomagnetic field variations*. Springer Science & Business Media.

Hansen, V. and Young, D. (2007). Venus's evolution: A synthesis. *Geological Society of America Special Papers*, 419:255–273.

Hansen, V. L. (2006). Geologic constraints on crustal plateau surface histories, venus: The lava pond and bolide impact hypotheses. *Journal of Geophysical Research: Planets (1991–2012)*, 111(E11).

Hansen, V. L., Banks, B. K., and Ghent, R. R. (1999). Tessera terrain and crustal plateaus, venus. *Geology*, 27(12):1071–1074.

Head, J. W., Crumpler, L., Aubele, J. C., Guest, J. E., and Saunders, R. S. (1992). Venus volcanism: Classification of volcanic features and structures, associations, and global distribution from magellan data. *Journal of Geophysical Research: Planets (1991–2012)*, 97(E8):13153–13197.

Herrick, R. R. (1994). Resurfacing history of venus. *Geology*, 22(8):703–706.

Herrick, R. R. and Phillips, R. J. (1994). Implications of a global survey of venusian impact craters. *Icarus*, 111(2):387–416.

Herrick, R. R. and Rumpf, M. E. (2011). Postimpact modification by volcanic or tectonic processes as the rule, not the exception, for venusian craters. *Journal of Geophysical Research: Planets (1991–2012)*, 116(E2).

Hofmeister, A. (1999). Mantle values of thermal conductivity and the geotherm from phonon lifetimes. *Science*, 283(5408):1699–1706.

Ivanov, M. and Head, J. (2014). Volcanically embayed craters on venus: testing the catastrophic and equilibrium resurfacing models. *Planetary and Space Science*.

James, P., Zuber, M., and Phillips, R. (2010). Geoid to topography ratios on venus and implications for crustal thickness. In *Lunar and Planetary Science Conference*, volume 41, page 2663.

Kargel, J., Komatsu, G., Baker, V., and Strom, R. (1993). The volcanology of venera and vega landing sites and the geochemistry of venus. *Icarus*, 103(2):253–275.

Konopliv, A., Banerdt, W., and Sjogren, W. (1999). Venus gravity: 180th degree and order model. *Icarus*, 139(1):3–18.

Konopliv, A. and Yoder, C. (1996). Venusian k2 tidal love number from magellan and pvo tracking data. *Geophysical research letters*, 23(14):1857–1860.

Korycansky, D. and Zahnle, K. (2005). Modeling crater populations on venus and titan. *Planetary and Space Science*, 53(7):695–710.

Kronbichler, M., Heister, T., and Bangerth, W. (2012). High accuracy mantle convection simulation through modern numerical methods. *Geophysical Journal International*, 191(1):12–29.

Marcq, E., Bertaux, J.-L., Montmessin, F., and Belyaev, D. (2013). Variations of sulphur dioxide at the cloud top of venus/'s dynamic atmosphere. *Nature geoscience*, 6(1):25–28.

Markiewicz, W., Titov, D., Ignatiev, N., Keller, H., Crisp, D., Limaye, S., Jaumann, R., Moissl, R., Thomas, N., Esposito, L., et al. (2007). Venus monitoring camera for venus express. *Planetary and Space Science*, 55(12):1701–1711.

Masursky, H., Eliason, E., Ford, P. G., McGill, G. E., Pettengill, G. H., Schaber, G. G., and Schubert, G. (1980). Pioneer venus radar results: Geology from images and altimetry. *Journal of Geophysical Research: Space Physics (1978–2012)*, 85(A13):8232–8260.

Mocquet, A., Rosenblatt, P., Dehant, V., and Verhoeven, O. (2011). The deep interior of venus, mars, and the earth: A brief review and the need for planetary surface-based measurements. *Planetary and Space Science*, 59(10):1048–1061.

Morgan, P. and Phillips, R. J. (1983). Hot spot heat transfer: Its application to venus and implications to venus and earth. *Journal of Geophysical Research: Solid Earth (1978–2012)*, 88(B10):8305–8317.

Mueller, N., Helbert, J., Erard, S., Piccioni, G., and Drossart, P. (2012). Rotation period of Venus estimated from Venus Express {VIRTIS} images and Magellan altimetry. *Icarus*, 217(2):474 – 483. Advances in Venus Science.

Namiki, N. and Solomon, S. C. (1994). Impact crater densities on volcanoes and coronae on venus: Implications for volcanic resurfacing. *Science*, 265(5174):929–933.

Oertel, D., Spänkuch, D., Jahn, H., Becker-Ross, H., Stadthaus, W., Nopirakowski, J., Döhler, W., Schäfer, K., Güldner, J., Dubois, R., et al. (1985). Infrared spectrometry of venus from venera-15 and venera-16. *Advances in Space Research*, 5(9):25–36.

O'Rourke, J. G., Wolf, A. S., and Ehlmann, B. L. (2014). Venus: Interpreting the spatial distribution of volcanically modified craters. *Geophysical Research Letters*.

Pettengill, G. H., Eliason, E., Ford, P. G., Loriot, G. B., Masursky, H., and McGill, G. E. (1980). Pioneer venus radar results altimetry and surface properties. *Journal of Geophysical Research: Space Physics (1978–2012)*, 85(A13):8261–8270.

Price, M. and Suppe, J. (1994). Mean age of rifting and volcanism on venus

deduced from impact crater densities.

Price, M. and Suppe, J. (1995). Constraints on the resurfacing history of venus from the hypsometry and distribution of volcanism, tectonism, and impact craters. *Earth, Moon, and Planets*, 71(1-2):99–145.

Rappaport, N. J., Konopliv, A. S., Kucinskas, A. B., and Ford, P. G. (1999). An improved 360 degree and order model of venus topography. *Icarus*, 139(1):19–31.

Romeo, I. (2013). Monte carlo models of the interaction between impact cratering and volcanic resurfacing on venus: The effect of the beta-atla-themis anomaly. *Planetary and Space Science*, 87:157–172.

Russell, C. T. (1976). The magnetic moment of venus: Venera-4 measurements reinterpreted. *Geophysical Research Letters*, 3(3):125–128.

Sagdeev, R., Linkin, V., Blamont, J., and Preston, R. (1986). The VEGA Venus balloon experiment. *Science*, 231(4744):1407–1408.

Schaber, G., Shoemaker, E., and Kozak, R. (1987). Surface age of Venus: use of the terrestrial cratering record. *Sol. Syst. Res.(Engl. Transl.);(United States)*, 21(2).

Schaber, G., Strom, R., Moore, H., Soderblom, L., Kirk, R., Chadwick, D., Dawson, D., Gaddis, L., Boyce, J., and Russell, J. (1992). Geology and distribution of impact craters on venus: What are they telling us? *Journal of Geophysical Research: Planets (1991–2012)*, 97(E8):13257–13301.

Schubert, G., Bercovici, D., and Glatzmaier, G. (1990). Mantle dynamics in mars and venus: Influence of an immobile lithosphere on three-dimensional mantle convection. *Journal of Geophysical Research: Solid Earth (1978–2012)*, 95(B9):14105–14129.

Schubert, G., Turcotte, D. L., and Olson, P. (2001). *Mantle Convection in the Earth and Planets 2 Volume Set*. Cambridge University Press.

Shalygin, E., Markiewicz, W., Basilevsky, A., Titov, D., Ignatiev, N., and Head, J. (2014). Bright transient spots in ganiki chasma, venus. In *Lunar and Planetary Institute Science Conference Abstracts*, volume 45, page 2556.

Simons, M., Solomon, S. C., and Hager, B. H. (1997). Localization of gravity and topography: Constraints on the tectonics and mantle dynamics of venus. *Geophysical Journal International*, 131(1):24–44.

Sjogren, W., Bills, B., Birkeland, P., Esposito, P., Konopliv, A., Mottinger, N., Ritke, S., and Phillips, R. (1983). Venus gravity anomalies and their correlations with topography. *Journal of Geophysical Research: Solid Earth (1978–2012)*, 88(B2):1119–1128.

Smrekar, S. E., Stofan, E. R., Mueller, N., Treiman, A., Elkins-Tanton, L., Helbert, J., Piccioni, G., and Drossart, P. (2010). Recent hotspot volcanism on venus from virtis emissivity data. *Science*, 328(5978):605–608.

Solomatov, V. (1995). Scaling of temperature-and stress-dependent viscosity convection. *Physics of Fluids (1994-present)*, 7(2):266–274.

Solomon, S. C. and Head, J. W. (1982). Mechanisms for lithospheric heat transport on venus implications for tectonic style and volcanism. *Journal of Geophysical Research*, 87:9236–9246.

Solomon, S. C., Smrekar, S. E., Bindschadler, D. L., Grimm, R. E., Kaula, W. M., McGill, G. E., Phillips, R. J., Saunders, R. S., Schubert, G., Squyres, S. W., et al. (1992). Venus tectonics: An overview of magellan observations. *Journal of Geophysical Research: Planets (1991–2012)*, 97(E8):13199–13255.

Steinbach, V. and Yuen, D. (1992). The effects of multiple phase transitions on venusian mantle convection. *Geophysical Research Letters*, 19(22):2243–2246.

Stofan, E. R., Sharpton, V. L., Schubert, G., Baer, G., Bindschadler, D. L., Janes, D. M., and Squyres, S. W. (1992). Global distribution and characteristics of coronae and related features on venus: Implications for origin and relation to mantle processes. *Journal of Geophysical Research: Planets (1991–2012)*, 97(E8):13347–13378.

Strom, R. G., Schaber, G. G., and Dawson, D. D. (1994). The global resurfacing of venus. *Journal of Geophysical Research: Planets (1991–2012)*, 99(E5):10899–10926.

Surkov, Y. A., Barsukov, V., Moskalyeva, L., Kharyukova, V., and Kemurdzhian, A. (1984). New data on the composition, structure, and properties of venus rock obtained by venera 13 and venera 14. *Journal of Geophysical Research: Solid Earth (1978–2012)*, 89(S02):B393–B402.

Surkov, Y. A., Kirnozov, F., Glazov, V., Dunchenko, A., Tatsy, L., and Sobornov, O. (1987). Uranium, thorium, and potassium in the venusian rocks at the landing sites of vega 1 and 2. *Journal of Geophysical Research: Solid Earth (1978–2012)*, 92(B4):E537–E540.

Surkov, Y. A., Moskalyeva, L., Shcheglov, O., Kharyukova, V., Manvelyan, O., Kirichenko, V., and Dudin, A. (1983). Determination of the elemental composition of rocks on venus by venera 13 and venera 14 (preliminary results). *Journal of Geophysical Research: Solid Earth (1978–2012)*, 88(S02):A481–A493.

Surkov, Y. A., Moskalyova, L., Kharyukova, V., Dudin, A., Smirnov, G., and Zaitseva, S. Y. (1986). Venus rock composition at the vega 2 landing site. *Journal of Geophysical Research: Solid Earth (1978–2012)*, 91(B13):E215–E218.

Svedhem, H., Titov, D., McCoy, D., Lebreton, J.-P., Barabash, S., Bertaux, J.-L., Drossart, P., Formisano, V., Häusler, B., Korablev, O., et al. (2007). Venus expressthe first european mission to venus. *Planetary and Space Science*, 55(12):1636–1652.

Titov, D., Svedhem, H., Koschny, D., Hoofs, R., Barabash, S., Bertaux, J.-L., Drossart, P., Formisano, V., Häusler, B., Korablev, O., et al. (2006). Venus express science planning. *Planetary and Space Science*, 54(13):1279–1297.

Tomasko, M., Doose, L., Palmer, J., Holmes, A., Wolfe, W., Castillo, N., and Smith, P. (1979). Preliminary results of the solar flux radiometer experiment aboard the pioneer venus multiprobe mission. *Science*, 203(4382):795–797.

Tosi, N., Stein, C., Noack, L., Hüttig, C., Maierová, P., Samuel, H., Davies, D., Wilson, C., Kramer, S., Thieulot, C., et al. (2015). A community benchmark for viscoplastic thermal convection in a 2-d square box. *Geochemistry, Geophysics, Geosystems*.

Trompert, R. and Hansen, U. (1998). Mantle convection simulations with rheologies that generate plate-like behaviour. *Nature*, 395(6703):686–689.

Turcotte, D. L. (1993). An episodic hypothesis for Venusian tectonics. *Journal of Geophysical Research: Planets (1991–2012)*, 98(E9):17061–17068.

Turcotte, D. L. (1995). How does Venus lose heat? *Journal of Geophysical Research: Planets (1991–2012)*, 100(E8):16931–16940.

van den Berg, A. P., Yuen, D. A., and Steinbach, V. (2001). The effects of variable thermal conductivity on mantle heat-transfer. *Geophysical Research Letters*, 28(5):875–878.

Vinogradov, A., Surkov, U., and Florensky, C. (1968). The chemical composition of the venus atmosphere based on the data of the interplanetary station venera 4. *Journal of the Atmospheric Sciences*, 25(4):535–536.

Vinogradov, A., Surkov, Y. A., and Kirnozov, F. (1973). The content of uranium, thorium, and potassium in the rocks of venus as measured by venera 8. *Icarus*, 20(3):253–259.

Watters, T. R. (1988). Wrinkle ridge assemblages on the terrestrial planets. *Journal of Geophysical Research: Solid Earth (1978–2012)*, 93(B9):10236–10254.

Yoder, C. F. (1995). Venus' free obliquity. *Icarus*, 117(2):250–286.

Zahnle, K. and McKinnon, W. B. (1996). Age of the surface of Venus. In *Bulletin of the American Astronomical Society*, volume 28, page 1119.